

Short title: GWAS/TWAS of stomatal closure in biomass sorghum

Corresponding author: Andrew D. B. Leakey: 217-244-0302, leakey@illinois.edu

Full title: Phenotyping stomatal closure by thermal imaging for GWAS and TWAS of water use efficiency-related genes

Charles P. Pignon^{1,2,3}, Samuel B. Fernandes^{2,3}, Ravi Valluru^{4,5}, Nonoy Bandillo^{4,6}, Roberto Lozano⁷, Edward Buckler^{7,8}, Michael A. Gore⁷, Stephen P. Long^{1,2,3,9}, Patrick J. Brown^{2,3}, Andrew D. B. Leakey^{1,3,4}

Affiliations:

¹Department of Plant Biology, University of Illinois at Urbana-Champaign, Urbana, IL 61801, USA.

²Department of Crop Sciences, University of Illinois at Urbana-Champaign, Urbana, IL 61801, USA.

³Carl R. Woese Institute for Genomic Biology, University of Illinois at Urbana-Champaign, Urbana, IL 61801, USA.

⁴Institute for Genomic Diversity, Cornell University, Ithaca, NY 14853, USA.

⁵Lincoln Institute for Agri-Food Technology, University of Lincoln, LN1 3QE Lincoln, UK.

⁶Department of Plant Sciences, North Dakota State University, Fargo, ND 58105, USA.

⁷Plant Breeding and Genetics Section, School of Integrative Plant Science, Cornell University, Ithaca, NY 14853, USA

⁸United States Department of Agriculture, Agricultural Research Service (USDA-ARS) R.W. Holley Center for Agriculture and Health, Ithaca, NY 14853, USA

⁹Lancaster Environment Centre, University of Lancaster, LA1 1YX, UK.

ORCID: 0000-0002-4237-1649 (C.P.P), 0000-0001-6896-8024 (M.A.G.), 0000-0003-1332-711X (P.J.B.), 0000-0001-6251-024X (A.D.B.L)

The author responsible for distribution of materials integral to the findings presented in this article in accordance with the policy described in the Instructions for Authors (<https://academic.oup.com/plphys/pages/General-Instructions>) is Andrew D. B. Leakey.

One sentence summary:

Dynamic stomatal responses to a decrease in light, measured in 659 *Sorghum bicolor* accessions, revealed substantial, heritable trait variation, associated with genes involved in water-use efficiency.

Footnotes:

Author contributions: The research was conceived by C.P., S.L., E.B., M.G. and A.L. Experiments were performed by C.P., P.B. and R.V.. Data was analyzed and interpreted by C.P., S.F., R.V., N.B., R.L. and A.L.. C.P. and A.L. wrote the paper with input from all authors. A.L. agrees to serve as the author responsible for contact and ensuring communication.

Funding information: This research was funded by the Advanced Research Projects Agency-Energy (ARPA-E), U.S. Department of Energy (DOE), under Award Number DE-AR0000661 and the Office of Biological and Environmental Research in the DOE Office of Science (DE-SC0018277). The views and opinions of authors expressed herein do not necessarily state or reflect those of the United States Government or any agency thereof.

Current addresses:

Pignon C: Benson Hill, 1005 N Warson Rd, St. Louis, MO 63132

Brown P: Department of Plant Sciences, University of California, Davis, CA 95616, USA.

Author for contact: leakey@illinois.edu

This manuscript is submitted as a Research Article

Abstract

Stomata allow CO₂ uptake by leaves for photosynthetic assimilation at the cost of water vapor loss to the atmosphere. The opening and closing of stomata in response to fluctuations in light intensity regulate CO₂ and water fluxes and are essential for maintaining water-use efficiency (WUE). However, little is known about the genetic basis for natural variation in stomatal movement, especially in C₄ crops. This is partly because the stomatal response to a change in light intensity is difficult to measure at the scale required for association studies. Here, we used high-throughput thermal imaging to bypass the phenotyping bottleneck and assess 10 traits describing stomatal conductance (g_s) before, during and after a stepwise decrease in light intensity for a diversity panel of 659 sorghum (*Sorghum bicolor*) accessions. Results from thermal imaging significantly correlated with photosynthetic gas-exchange measurements. g_s traits varied substantially across the population and were moderately heritable (h^2 up to 0.72). An integrated genome-wide and transcriptome-wide association study (GWAS/TWAS) identified candidate genes putatively driving variation in stomatal conductance traits. Of the 239 unique candidate genes identified with greatest confidence, 77 were putative orthologs of Arabidopsis (*Arabidopsis thaliana*) genes related to functions implicated in WUE, including stomatal opening/closing (24 genes), stomatal/epidermal cell development (35 genes), leaf/vasculature development (12 genes), or chlorophyll metabolism/photosynthesis (8 genes). These findings demonstrate an approach to finding genotype-to-phenotype relationships for a challenging trait as well as candidate genes for further investigation of the genetic basis of WUE in a model C₄ grass for bioenergy, food, and forage production.

Introduction

Water availability is a major limiting factor to agriculture worldwide (Boyer, 1982), and is predicted to become even more limiting due to rising demand for water resulting from increasing atmospheric vapor pressure deficit (VPD) with climate change (Lobell et al., 2008; WWAP, 2015; FAO et al., 2018). Greater crop water use associated with greater above-ground biomass has also been implicated in past and future increases in crop yield (Sinclair et al., 1984; Ray et al., 2013; Lobell et al., 2014; Ort and Long, 2014; Koester et al., 2016; DeLucia et al., 2019). Therefore, unless WUE is enhanced, agricultural systems in the near future will be increasingly threatened by drought, and unsustainable practices such as over-irrigation may result (DeLucia et al., 2019; Leakey et al., 2019).

WUE is key to terrestrial plant growth due to the inherent trade-off between net photosynthetic carbon assimilation (A) and water loss through transpiration (Wong et al., 1979). Most leaf water and CO_2 fluxes pass through stomatal pores (Kerstiens, 1996; Hetherington and Woodward, 2003). Stomatal aperture is dynamically regulated by the movement of stomatal guard cells (Assmann and Jegla, 2016), which respond to extrinsic and intrinsic signals to optimize CO_2 uptake relative to water vapor loss (Medlyn et al., 2011). The synchrony of stomatal opening and closing with fluctuations in photosynthetic CO_2 assimilation varies within and among species, with significant consequences for intrinsic water-use efficiency ($iWUE$, the ratio of A to stomatal conductance to water vapor (g_s)) (Lawson and Blatt, 2014; Kaiser et al., 2015). If conditions are favorable for A , but g_s is low, A will be limited by CO_2 supply. Conversely, if A is low, but g_s is high, unnecessary transpiration will occur with no corresponding benefit to A , substantially decreasing $iWUE$. This is important in fluctuating light environments such as field crop canopies, where the movement of clouds and leaves cause frequent and abrupt changes in photosynthetic photon flux density ($PPFD$) at the leaf level (Percy, 1990; Zhu et al., 2004; Way and Percy, 2012; Wang et al., 2020).

Generally, g_s responds an order of magnitude more slowly than A to a decline in $PPFD$, declining to a new steady-state over the course of several minutes (Hetherington and Woodward, 2003; McAusland et al., 2016). This results in a de-synchronization of A and g_s and loss of $iWUE$. Ensuring that A and g_s are synchronized in their response to fluctuating light, by accelerating stomatal movement, could yield substantial benefits to $iWUE$ of 20-30% (Lawson

and Blatt, 2014). Proof-of-concept from transgenic manipulation of the stomatal light-sensing mechanism has led to accelerated stomatal movement and improved *iWUE* in fluctuating light in *Arabidopsis* (*Arabidopsis thaliana*) and *Nicotiana benthamiana* (Papanatsiou et al., 2019). Still, accelerating stomatal movement by breeding or biotechnology for improved *iWUE* remains an open challenge in cereal crops (Faralli et al., 2019).

The genetic basis for natural variation in traits describing stomatal opening/closing is poorly understood, in part because such traits are difficult to phenotype at the scale required for association studies. The response of g_s to fluctuating light is lengthy, with some species needing >30 minutes to transition from steady-state at one light intensity to another (Lawson and Blatt, 2014; McAusland et al., 2016; Deans et al., 2019). The standard measurement of g_s using gas-exchange chambers or porometers requires a single instrument for each leaf, so is costly in terms of personnel and equipment. Using thermal imaging to track changes in leaf temperature resulting from stomatal movement, with the leaf warming up as stomata close due to a proportionate reduction of cooling by transpiration, provides a high throughput phenotyping method in which numerous leaves can be measured simultaneously (Jones et al., 2002; Guillioni et al., 2008; Violet-Chabrand and Lawson, 2019). Thermal imaging has been used to monitor stomatal closure (Jones et al., 2002) and stress response (Grant et al., 2007) in a grapevine field, to identify *Arabidopsis* mutants with altered g_s (Merlot et al., 2002), and coupled with chlorophyll fluorescence measurements to screen *Arabidopsis* plants for *iWUE* (McAusland et al., 2013). In a broad validation experiment, thermal measurements predicted g_s for a range of species exposed to different experimental treatments (Grant et al., 2006). Finally, thermal imaging was used to perform high-throughput phenotyping of the response of hundreds of ecotypes of *Arabidopsis* to changing light and $[CO_2]$ (Takahashi et al., 2015). However, the ability of thermal imaging to produce trait estimates with sufficiently high heritability to support quantitative genetic investigation of genotype-to-phenotype relationships for stomatal opening/closing remains unclear.

Genome-wide association studies (GWAS) are widely used to identify the genetic basis for natural variation in agronomic, developmental, physiological and biochemical traits in plant species, including sorghum (*Sorghum bicolor*) (Casa et al., 2008; Morris et al., 2013; Burks et al., 2015; Ortiz et al., 2017). The benefits and limitations of the approach have been reviewed in

many contexts (Liu and Yan, 2019; Tam et al., 2019; Zhou and Huang, 2019). GWAS of stomatal movement can be challenging because biophysical trade-offs can limit the extent of natural variation in the trait, for instance because the speed of stomatal movement is constrained by the dimensions and patterning of stomata, which in turn are linked to leaf development and photosynthetic capacity. Measurements may also be slow, sensitive to environmental conditions, and lack accuracy, precision, or both. Together, these factors can reduce the variance that can be ascribed to genotype, i.e. reduce heritability, and constrain the size of the mapping population that can be studied, resulting in low statistical power. Recently, combining GWAS with transcriptome-wide association study (TWAS), which identifies significant associations between trait variation and RNA transcript abundance across all expressed genes in a tissue, has been shown to improve identification of genes underlying trait variation (Kremling et al., 2019).

This study aimed to demonstrate how phenotyping by thermal imaging could be used in conjunction with integrated GWAS/TWAS to quantify natural diversity in stomatal/opening closing and identify genotype-to-phenotype relationships in a model *C₄* crop. *Sorghum bicolor* ((L.) Moench) is a model species used to study photosynthesis, abiotic/biotic stress and canopy architecture, as well as applied investigations in the context of food, fuel and forage production (Paterson et al., 2009; Morris et al., 2013). It has particular importance in semi-arid conditions due to its high productivity and drought-tolerance (Regassa and Wortmann, 2014; Hadebe et al., 2017). Sorghum is an especially interesting model in which to study stomatal movement because it has fast stomatal responses to decreasing light relative to other species (McAusland et al., 2016; Pignon et al., 2021). High-throughput thermal imaging was used to measure 10 traits describing the response of g_s to a decrease in photosynthetic photon flux density (*PPFD*) in over 2000 plants of 659 accessions in a sorghum association mapping population. Results were validated against photosynthetic gas-exchange measurements. Phenotypic trait correlations were used to identify general patterns in stomatal behavior. GWAS and TWAS were performed to identify phenotype to genotype associations, along with an ensemble approach combining GWAS and TWAS results using the Fisher's combined test (FCT) (Kremling et al., 2019), followed by a GO enrichment analysis. The resulting list of 239 candidate genes identified with greatest confidence was enriched in putative orthologs of genes implicated in stomatal and photosynthetic traits in *Arabidopsis* and maize.

Results

Leaf temperature is affected by g_s , because leaves with increased g_s will undergo greater evaporative cooling and have a lower temperature as a result. However, leaf temperature may also be affected by environmental factors including air temperature, air flow, incident light, and leaf angle. To minimize these confounding effects, thermal imaging was performed in a temperature-controlled chamber, and leaf angle was standardized across all plants. Wet and dry reference materials were used to account for environmental effects on leaf temperature. Temperatures of leaves and reference materials were used to estimate g_s from thermal imaging, i.e. $g_{s\text{ thermal}}$.

The response of $g_{s\text{ thermal}}$ to a reduction in $PPFD$ from 750 to 75 $\mu\text{mol m}^{-2} \text{s}^{-1}$ was measured in 659 sorghum accessions (Table 1; Fig. 1). On a subset of 64 plants, g_s estimates were also obtained from gas-exchange measurements to validate $g_{s\text{ thermal}}$ as a proxy for g_s . Both $g_{s\text{ thermal}}$ and g_s predicted a similar pattern of stomatal closure upon a decrease in $PPFD$, sometimes followed by re-opening at low $PPFD$ (Fig. 2). All traits derived from $g_{s\text{ thermal}}$ were significantly and positively correlated with their equivalents from g_s ($p < 0.005$, Pearson's r ranging from 0.38 - 0.59, Spearman's rank-order ρ ranging from 0.29 - 0.66, Fig. 3).

Genetic variation, heritability, and trait correlations

Variation among accessions was 3-fold, 10-fold, 6-fold, and 8-fold, respectively, for steady-state $g_{s\text{ thermal}}$ at high $PPFD$ ($g_{s\text{ light}}$), steady-state $g_{s\text{ thermal}}$ at low $PPFD$ ($g_{s\text{ shade}}$), the amplitude of decline in $g_{s\text{ thermal}}$ from high to low $PPFD$ ($g_{s\text{ light}} - g_{s\text{ shade}}$), and integrated $g_{s\text{ thermal}}$ throughout the low- $PPFD$ period ($g_{s\text{ } \Sigma \text{ shade}}$, Table 1). For example, $g_{s\text{ light}}$ in accession PI552851 was more than double that of accession PI267653 (Fig. 4A-B). After the decrease in $PPFD$, $g_{s\text{ thermal}}$ declined at an exponential rate (V_{initial}), then reached a minimum ($g_{s\text{ initial min}}$), and the time to reach this minimum was recorded ($t_{\text{initial min}}$). Variation among accessions was 28-fold, 9-fold, and 7-fold, respectively, for V_{initial} , $g_{s\text{ initial min}}$, and $t_{\text{initial min}}$, respectively (Table 1). For example, the decline of $g_{s\text{ thermal}}$ was faster in PI267653, which displayed a strongly negative V_{initial} and low $t_{\text{initial min}}$ relative to slower accessions such as PI552851 (Fig. 4A-B). Stomatal re-opening often occurred after the initial decline causing a dampened oscillation in $g_{s\text{ thermal}}$ during adjustment to low $PPFD$. The variation among accessions was 37-fold, 7-fold, and 9-fold, respectively, for the linear increase in $g_{s\text{ thermal}}$ ($V_{\text{oscillation}}$), $g_{s\text{ thermal}}$ at peak stomatal re-opening ($g_{s\text{ oscillation max}}$) and the

amplitude of oscillation ($g_{s \text{ oscillation max}} - g_{s \text{ initial min}}$). For example, the oscillation of $g_{s \text{ thermal}}$ was more pronounced in NSL50717, which displayed high $V_{\text{oscillation}}$ and high oscillation amplitude ($g_{s \text{ oscillation max}} - g_{s \text{ initial min}}$), relative to PI660605, which showed no stomatal re-opening (Fig. 4C-D). Oscillation of $g_{s \text{ thermal}}$ occurred on different timescales, e.g. more protracted in PI329646 than PI660630 (Fig. 4E-F). Variation in these traits among genotypes was reproducible across replicates (Fig. 4A-F).

Genomic heritability (h^2) was highest (0.67-0.72) in traits describing $g_{s \text{ thermal}}$ at low $PPFD$, including $g_{s \text{ initial min}}$, $g_{s \text{ oscillation max}}$, $g_{s \text{ shade}}$, and $g_{s \Sigma \text{ shade}}$ (Table 1). Traits describing the speed of change in $g_{s \text{ thermal}}$ after a decrease in $PPFD$ (V_{initial} , $t_{\text{initial min}}$) also had moderately high h^2 (0.67-0.68). Traits describing the oscillation in $g_{s \text{ thermal}}$ during stomatal re-opening at low $PPFD$ ($V_{\text{oscillation}}$, $g_{s \text{ oscillation max}} - g_{s \text{ initial min}}$) had low to intermediate h^2 (0.24-0.49). h^2 was low (0.31) in traits describing $g_{s \text{ thermal}}$ at high $PPFD$ and the amplitude of overall decline in $g_{s \text{ thermal}}$ from high to low $PPFD$: $g_{s \text{ light}}$ and $g_{s \text{ light}} - g_{s \text{ shade}}$, respectively.

All traits were correlated (r from -0.29 – 0.94) with one another ($p < 0.05$, Fig. 5, Supplemental Fig. S1). In particular, accessions with high $g_{s \text{ thermal}}$ at high $PPFD$ also had greater overall $g_{s \text{ thermal}}$ at low $PPFD$ (positive correlation of $g_{s \text{ light}}$ and $g_{s \Sigma \text{ shade}}$, $p < 0.0001$, $r = 0.58$, Fig. 6A), took longer to adjust to the decrease in $PPFD$ (positive correlation of $g_{s \text{ light}}$ and $t_{\text{initial min}}$, $p < 0.0001$, $r = 0.3$; positive correlation of $g_{s \text{ light}}$ and V_{initial} , $p < 0.0001$, $r = 0.34$, Fig. 6B-C), and had more pronounced stomatal re-opening at low $PPFD$ (positive correlation of $g_{s \text{ light}}$ and $V_{\text{oscillation}}$, $p < 0.0001$, $r = 0.21$, Fig. 6D).

GWAS, TWAS, FCT and GO enrichment analysis

For each $g_{s \text{ thermal}}$ trait, genes were initially identified as of potential interest if they were in linkage disequilibrium (LD) (Supplemental Table S1) with the top 0.1% strongest associated SNPs from GWAS (~600 genes per trait; Supplemental Tables S2 & S9); among the top 1% strongest associated genes from TWAS for leaf or shoot tissues (169 and 199 genes per trait, respectively; Supplemental Table S3); or among the top 1% strongest associated genes from FCT for leaf or shoot tissues (150 genes per trait; Supplemental Table S4). In addition to individual traits, multi-trait associations were performed with two trait groups: G1) traits describing the speed of change in $g_{s \text{ thermal}}$ after a decrease in $PPFD$ (V_{initial} , $t_{\text{initial min}}$), and G2) traits describing

overall values of $g_{s\text{ thermal}}$ ($g_{s\text{ light}}$, $g_{s\text{ initial min}}$, $g_{s\text{ oscillation max}}$, $g_{s\text{ shade}}$, $g_{s\text{ } \Sigma\text{ shade}}$). The compilation of these results (Table S5) indicated that there was substantial overlap in genes identified for different $g_{s\text{ thermal}}$ traits, with 37% of genes being identified for two or more traits (Table 2).

Follow-up analyses were also performed to identify a subset of “higher confidence” genes, i.e. genes for which there was evidence for an association of trait variation with DNA sequence variation (GWAS) and RNA transcript abundance (TWAS), or genes identified in tests from both of the two independent approaches to sampling developing leaf tissue, i.e. from the 3rd *leaf* or *shoot* section containing the growing point. Therefore, genes overlapping the top hits for multiple analyses/tissues, i.e. GWAS, TWAS leaf, TWAS shoot, FCT leaf, and/or FCT shoot (n. overlaps ≥ 2 in Supplemental Table S5), were further investigated (Supplemental Fig. S2-S12). Across all traits, 1548 candidate genes were identified consistently across two or more of the individual tests. Taking V_{initial} as a representative trait, of the 1007 top hits, 180 were identified from at least two analyses/tissues (Fig. 7).

GO enrichment analysis on Arabidopsis putative orthologs of the “higher confidence” genes identified 153 significantly enriched biological processes (FDR-adjusted $p < 0.05$), nested within 34 broad categories (Supplemental Table S6). Among these, 22 categories of biological processes (e.g. *regulation of histone H3-K27 methylation*, *hydrogen peroxide metabolic process*, *cell cycle DNA replication*, *plant epidermis morphogenesis*, *lipid catabolic process* and *plant-type cell wall biogenesis*) were enriched by > 2.5 -fold (Fig. 8). A total of 239 unique genes contained within these GO categories were considered the strongest candidates to underlie variation in stomatal conductance traits studied here. A survey of the literature on their putative orthologs in Arabidopsis, maize and rice revealed a large proportion of genes (32 %) had functions related to stomatal opening/closing (24 genes), stomatal/epidermal cell development (35 genes), leaf/vasculature development (12 genes), or chlorophyll metabolism/photosynthesis (8 genes) (Supplemental Table S7). The positive or negative relationship between transcript abundance and trait variation was indicated by the TWAS (Table S3).

Discussion

Stomatal responses to changes in *PPFD* influence WUE of plants in fluctuating light environments (Lawson and Blatt, 2014). This study met the objectives of: (1) demonstrating how high-throughput thermal imaging can be used to rapidly phenotype variation in stomatal closure responses to *PPFD* across a diverse population of C_4 plants; and (2) using that data to perform an integrated GWAS/TWAS that identified a compelling set of candidate genes for further investigation of stomatal opening and closing in C_4 species. Thermal measurements were validated against classical gas-exchange, and phenotypic correlations revealed relationships between steady-state (e.g. g_s *light*) and dynamic (e.g. $V_{initial}$) stomatal conductance traits. Results showed substantial, heritable variation in dynamic responses of stomata to a reduction in *PPFD*. This study presents important information on sorghum, a model system with rapid stomatal movement compared to other species (McAusland et al., 2016), and addresses a major knowledge gap that exists for C_4 species, despite their agricultural and ecological importance (Edwards et al., 2010; Leakey et al., 2019).

Validation of $g_{s\ thermal}$ as a high-throughput proxy for g_s

Although dynamic g_s responses have been increasingly studied in the past few years (McAusland et al., 2016; Deans et al., 2019; Acevedo-Siaca et al., 2020; De Souza et al., 2020; Pignon et al., 2021), measurements have not yet been deployed at a scale amenable to association mapping (e.g., GWAS). Here, $g_{s\ thermal}$ was a useful high-throughput proxy for g_s , enabling simultaneous measurement of 18 plants in a single imaging frame. Previous studies have reported near-perfect correlation between $g_{s\ thermal}$ and g_s when g_s varied by more than an order of magnitude as a result of combining data from multiple *PPFD*s, species, genotypes and mutants (Spearman's rank-order $\rho=0.96$) (McAusland et al., 2013). In contrast, the present study focused on testing the correlations between estimates of individual traits measured by photosynthetic gas exchange versus thermal imaging when considering only natural genetic variation within a single species. For example, thermal imaging was highly significant ($p<0.001$) in capturing variation in g_s measured by gas exchange at a single *PPFD* (ρ ranging from 0.29 - 0.66, Fig. 3) and the thermal estimate of $g_{s\ shade}$ had a heritability of 0.70, making it suitable for association mapping. It is also notable that correlations between the two measurement approaches would have been weakened because $g_{s\ thermal}$ and g_s were not measured simultaneously in the manner achieved by

McAusland et al. (2013). For example, consistency between the two approaches to g_s measurements was likely reduced by differences in measurement conditions and the immediate history of environmental conditions experienced by leaves as they moved from thermal measurements to the gas exchange chamber. Boundary layer conductance was likely lower while measuring $g_{s\text{ thermal}}$ than g_s due to the air mixing fan used in gas-exchange equipment (Grant et al., 2006). Light quality was equal parts red/blue/green for $g_{s\text{ thermal}}$ vs. 90% red 10% blue for g_s . This likely affected stomatal opening, which is induced by blue, and to a lesser extent, red light (Assmann and Shimazaki, 1999; Shimazaki et al., 2007; Lawson et al., 2011; Assmann and Jegla, 2016). For these reasons, the significant correlations between all traits estimated from $g_{s\text{ thermal}}$ and their counterparts estimated from gas exchange measurements were considered a validation of the methods used.

There is potential for further advancing the rapid phenotyping of photosynthesis and water relations under dynamic environments. In a precisely controlled environment, measurements of thermal transients could easily be scaled beyond the 18 plants measured simultaneously here, either by using multiple cameras, or by using higher-resolution cameras placed higher above the plants. And, there is significant value in simultaneously imaging chlorophyll fluorescence and leaf temperature (McAusland et al. 2013). Although, great care and possibly technical advances will be needed to insure homogeneous illumination across all samples when scaling up either imaging modality. Transient thermal measurements may also complement other imaging tools used to assess plant water status in controlled environments, such as analysis of plant shape and color using RGB imaging (Fahlgren et al., 2015). In general, effective screening of stomatal dynamics is most practical in controlled environment settings due to greater control of environmental conditions and also the manner in which plants are pre-conditioned prior to data collection. But, thermal cameras mounted on aircraft, gantries and cable-systems, or used from boom lifts, have enabled reliable field-scale measurements of plant temperature (Deery et al., 2016; Deery et al., 2019; Sagan et al., 2019), including for identification of QTL that overlap with stomatal density QTL (Prakash et al., 2021), but in these settings the changes in leaf temperature caused by dynamic stomatal changes coincide with the transient effects of wind, leaf shading, and leaf angle. So, evaluating dynamic stomatal responses to varying PPFD in the field remains a daunting prospect.

Sorghum shows varied, heritable stomatal responses to a decrease in *PPFD*

Within-species diversity in stomatal light responses has been documented for C_3 species including *Arabidopsis* (Takahashi et al., 2015), poplar (Durand et al., 2019), rice (Acevedo-Siaca et al., 2020), cassava (De Souza et al., 2020) and soybean (Soleh et al., 2016). Expanding the scale of investigation to 659 accessions of sorghum revealed substantial variation within the C_4 model species, despite the fact that C_4 species generally have lower g_s than C_3 species (Taylor et al., 2010). The range of $t_{initial\ min}$ shown here (1.8-13.4 minutes, Table 1) overlapped with similar measurements in sorghum (~2-8 minutes) (McAusland et al., 2016; Pignon et al., 2021), the closely related C_4 grasses *miscanthus* and maize (~8 minutes), the C_3 grass rice (~10 minutes) (McAusland et al., 2016), and the semi-aquatic rhizomatous fern *Marsilea drummondii* A. Braun (~9 minutes) (Deans et al., 2019). Some C_3 dicots such as *Arabidopsis* and sunflower (~18 minutes) were roughly comparable to the slowest accession shown here ($t_{initial\ min} = 13.4$ minutes), while many other species appeared considerably slower (~30 minutes) (McAusland et al., 2016; Deans et al., 2019). The faster stomata of sorghum might be related to the unique structure of graminaceous stomata, composed of dumbbell-shaped guard cells flanked by subsidiary cells, which have been linked to rapid movement relative to other forms (Franks and Farquhar, 2007; Lawson et al., 2011; Serna, 2011; McAusland et al., 2016; Lawson and Vialet-Chabrand, 2019). Stomata of C_4 plants tend to be smaller and more sensitive to environmental change than their C_3 counterparts (Lawson et al., 2011; McAusland et al., 2016).

Implications of natural diversity in stomatal responses to decreasing *PPFD*

Variation within and among accessions in $g_{s\ thermal}$ could be observed at different stages of the light to dark-transition (Fig. 4), which was captured effectively by the steady-state and dynamic traits extracted from thermal transients (Fig. 1) resulting in generally high h^2 (Table 1). Compared to steady-state g_s under high *PPFD*, traits describing the dynamic change in $g_{s\ thermal}$ after a decrease in *PPFD* had greater variability and h^2 , making them more tractable targets for association studies (Table 1). Additionally, variation in traits describing the speed of change in $g_{s\ thermal}$ after a decrease in *PPFD* ($V_{initial}$, $t_{initial\ min}$) might be leveraged to accelerate stomatal responses even in species with “fast” stomata such as sorghum, potentially improving coordination of g_s with photosynthetic carbon assimilation (A) and resulting in improved *iWUE* (Lawson and Blatt, 2014). Other traits ($V_{oscillation}$, $g_{s\ oscillation\ max} - g_{s\ initial\ min}$) described stomatal

oscillations similar to those observed in other species, especially when blue light is applied (Ballard et al., 2019) and when stomatal apertures are low (Kaiser and Kappen, 2001). However, the stomatal oscillations observed in our study occurred on a lengthy timescale (up to 1 hour), and are unlikely to substantially impact *iWUE* of field crop stands, where most light fluctuations last on the order of seconds (Kaiser et al., 2018).

The relationships among traits observed across the genetic variation surveyed here are consistent with biophysical trade-offs driven by structure-functional relationships, as well as selection for trait combinations that favor carbon gain versus water savings to differing degrees in different environments. The finding that accessions with greater $g_{s\ light}$ took longer to adjust to decreasing *PPFD* (Fig. 6B-C) is supported by similar patterns across diverse species (McAusland et al., 2016), and is consistent with greater $g_{s\ light}$ being associated with greater stomatal apertures requiring more time to close (Lawson and Blatt, 2014). However, it is worth noting that variation in stomatal opening/closing is also associated with guard cell physiology, including ion transport processes (Lawson and Blatt 2014). Adaptation to different environments may also contribute to the observed trait correlations, with high $g_{s\ light}$ and slow stomatal closure working in concert to favor *A* and rapid growth in environments where water is not limiting. In contrast, low $g_{s\ light}$ and rapid stomatal closure combine to prioritize water-use efficiency and conservative but sustained growth in water-limited environments (Vico et al., 2011). Since more rapid stomatal closure after a decrease in *PPFD* would increase *iWUE*, there is significant interest in identifying more genes underpinning structural and functional components of stomatal movements, as well as their interactions with steady-state gas exchange and leaf development and physiology more broadly (Lawson and Blatt 2014).

The number of stomata per unit leaf area, dimensions of stomata, extent of opening, and arrangement of stomata on the leaf surface all influence g_s (Dow et al., 2014; Faralli et al., 2019). Three of these four factors are anatomical features that are fixed during leaf development (Serna, 2011; Nunes et al., 2020). In addition, guard cell movement allows variation of the stomatal aperture in response to environmental signals including light intensity and spectral composition (Assmann and Jegla, 2016), $[CO_2]$ (Assmann and Jegla, 2016) and leaf-to-air vapor pressure deficit (Ball et al., 1987; McAdam and Brodribb, 2015). Therefore, many biological processes, pathways and genes can influence g_s . This study advanced understanding of these factors through

a GWAS/TWAS approach used to identify the most influential genes underlying phenotypic variation in *g_s thermal* traits.

GWAS/TWAS identifies genes enriched in stomatal, leaf developmental and photosynthetic functions

Gene candidates putatively associated with genetic variation in stomatal closure in sorghum were identified using GWAS and TWAS integrated with FCT, followed by GO enrichment analysis. This approach has identified known causal variants more efficiently than GWAS and TWAS alone (Kremling et al., 2019), while also increasing the consistency in results observed when testing was repeated across different conditions (Ferguson et al., 2021). The present study reinforced these prior reports, with an order of magnitude more genes being consistently identified by FCT versus TWAS across the two independent tissue sampling strategies used (Supplemental Table S5). GO enrichment analysis of the Arabidopsis putative orthologs of these genes revealed 22 GO biological processes that were significantly and >2.5-fold enriched (Supplemental Table S6, Fig. 8). The 239 genes belonging to these 22 categories were selected as the greatest confidence candidate genes (Fig. 8; Supplemental Table S7). A large proportion (32%) of these genes have putative orthologs in Arabidopsis, maize or rice that are already implicated in regulating traits related to stomata or WUE. While it is unlikely that such enrichment would occur by random chance, the function of the genes identified here will require confirmation by follow-up reverse genetic studies of transgenic or mutant plants. Examples of genes discovered through the GWAS/TWAS are described below in three categories corresponding to genes involved in: (i) guard cell signaling, metabolism or transport; (ii) stomatal or epidermal patterning; and (iii) overall leaf development, vasculature and photosynthesis.

Twenty three putative orthologs of genes implicated in signaling, metabolism or transporters in guard cells belong to enriched GO terms including *hydrogen peroxide metabolic process*, *response to disaccharide*, *response to heat*, and *lipid catabolic process* (Supplemental Table S7). For example, loss of ASCORBATE PEROXIDASE 1 (APX1) and the RESPIRATORY BURST OXIDASE HOMOLOG PROTEIN F (RBOHF) influence redox oxygen species (ROS) to alter stomatal responses to light, [CO₂] or abscisic acid (ABA; Pnueli et al., 2003; Chater et al., 2015; Sierla et al., 2016). The TWAS revealed that lower APX1 transcript abundance in developing

leaf tissues in a sorghum accession was associated with slower stomatal closure (APX1 putative ortholog SOBIC.001G410200 in traits $V_{initial\ min}$ & $t_{initial\ min}$, Table S3), which is a more subtle version of the severe impairment of stomatal movements observed in knockout-APX1 plants of Arabidopsis (Pnueli et al., 2003). Meanwhile, the MYB60 transcription factor is required for light induced opening of stomata in Arabidopsis. It is expressed exclusively in guard cells, with expression increasing and decreasing in accordance with conditions that promote stomatal opening and closing, respectively (Cominelli et al., 2005). This is consistent with the observation that sorghum accessions with greater MYB60 transcript abundance in the shoot growing point closed their stomata more rapidly after a decrease in PPFD (MYB60 putative ortholog SOBIC.005G155900 in trait $t_{initial\ min}$, Supplemental Table S3). Other genes identified that have putative orthologs in Arabidopsis that are involved in guard cell metabolism or signaling included PHOSPHOLIPASE D α 1 (PLD α 1), which along with its lipid product phosphatidic acid, impacts ABA-induction of ROS production and stomatal closure (Zhang et al., 2009). Mutants of ABC TRANSPORTER G FAMILY MEMBER 40 (ABCG40) shut more slowly in response to ABA (Kang et al., 2010), while its sorghum putative ortholog was variously associated with 5 different g_s thermal traits in GWAS, TWAS and FCT tests.

Recently, lipid metabolism of guard cells was discovered to be important as an energy source for light-induced stomatal opening (McLachlan et al., 2016). Five sorghum genes associated with variation in g_s thermal traits were putative orthologs of genes involved in triacyl glyceride mobilization and expressed in guard cells of Arabidopsis (ENOYL-COA DELTA ISOMERASE 1 and 3, ECI1 and ECI3; PEROXISOMAL FATTY ACID BETA-OXIDATION MULTIFUNCTIONAL PROTEIN, MFP2; ACYL-COENZYME A OXIDASE 2 and 4, ACX2 and ACX4; McLachlan et al., 2016). Notably, WRINKLED1, a transcription factor that regulates metabolic genes in a manner that promotes carbon allocation to fatty acid synthesis, was also identified (Cernac and Benning, 2004). Overall, a substantial proportion of the highest confidence candidate genes identified by the integrated GWAS/TWAS are plausibly involved in signaling, metabolism and transport functions in guard cells. Further study will be needed to determine if the candidate genes identified here play specific roles in stomatal closure, or if the associations observed in this study are partly a product of the strong correlations between rates of stomatal opening and closing (Lawson and Blatt, 2014). Current understanding of lipid

metabolism guard cells would seem to suggest the latter option is more likely, but this area of study is still relatively nascent.

The functions of putative orthologs of the highest confidence sorghum candidate genes are also consistent with the importance of stomatal size, density and distribution to the speed of stomatal opening and closing. Thirty five putative orthologs of genes implicated in stomatal or epidermal cell patterning belong to enriched GO terms including *plant epidermis morphogenesis*, *cell cycle DNA replication*, *plant-type cell wall biogenesis*, and *plastid organization* (Supplemental Table S7). Arabidopsis genes known to impact stomatal development or patterning which had sorghum putative orthologs found in the highest confidence candidates for *g_s thermal* traits included: MAP KINASE KINASE KINASE 4 (YODA, Bergmann et al., 2004); the FAMA bHLH-type transcription factor (Ohashi-Ito and Bergmann, 2006), CYCLIN-DEPENDENT KINASE B1;1, (CDKB1;1, Boudolf et al., 2004); PHYTOCHROME INTERACTING FACTOR 1 (PIF1, Klarmund et al., 2016), SOMATIC EMBRYOGENIC RECEPTOR KINASE 1 (SERK1, Meng et al., 2015), DNA-DIRECTED RNA POLYMERASE II SUBUNIT 2 (NRPB2; Chen et al., 2016), CHROMATIN REGULATOR ENHANCED DOWNY MILDEW 2 (EDM2, Wang et al., 2016), PROTEIN PHOSPHATASE 2A (Bian et al., 2020), GATA, NITRATE-INDUCIBLE, CARBON METABOLISM-INVOLVED (GNC, Klarmund et al., 2016), EXTRA-LARGE GTP-BINDING PROTEIN (XLG3, Chakravorty et al., 2015), and ARF GUANINE-NUCLEOTIDE EXCHANGE FACTOR (GNOM, Le et al., 2014). Sorghum accessions with lower NRPB2 transcript abundance in developing leaf tissue had greater *g_s* at high light (NRPB2 putative ortholog SOBIC.001G155000 in trait *g_s light*, Supplemental Table S3), which is consistent with a positive correlation between stomatal density and *g_s* (Pignon et al., 2021) and NRPB2 loss-of-function mutants having greater SD (Chen et al., 2016). Meanwhile, stomata closed more rapidly in accessions with lower abundance of EDM2 transcripts in developing leaf tissue (EDM2 putative ortholog SOBIC.002G154000 in trait *t_{initial min}*, Supplemental Table S3). This is consistent with bigger stomata having slower movements, occurring when stomatal density is low (Pignon et al., 2021) and EDM2 loss-of-function mutants having greater stomatal density (Wang et al., 2016).

Focusing on putative orthologs in other grasses, SOBIC.010G277300 shares 96 % predicted protein sequence similarity with GRMZM2G057000 in maize. The *nana plant2* (na2)

mutant of this gene displays alterations in brassinosteroid synthesis and the morphology of stomatal complexes (Best et al., 2016). Similarly, SOBIC.004G116400 shares 74 % predicted protein sequence similarity with Os02g15950 (ERECT PANICLE 3, EP3) in rice (*Oryza sativa*). Loss of function mutants of EP3 have smaller stomata, which appeared to drive reductions in g_s and A (Yu et al., 2015). Given the substantial evidence for links between gas exchange, stomatal complex size and stomatal density (Lawson and Blatt 2014; Xie et al., 2020), there is potential for variations in the sequence and expression of these genes to drive variation in the g_s thermal traits measured in this study. A number of other genes identified by the integrated GWAS/TWAS have been implicated in the development of epidermal cells in general (Supplemental Table S7). Cross talk between development pathways for stomata and other types of epidermal cells (Kim and Dolan, 2011; Raissig et al., 2016) creates the opportunity for such genes to influence g_s and its response to *PPFD*.

Finally, a smaller number of sorghum genes identified in this study have putative orthologs known to influence overall *leaf development/vasculature* (9 genes) or *chlorophyll/photosynthesis* (7 genes) (Supplemental Table S7). Leaf vasculature determines the hydraulic capacity of the leaf to deliver water that eventually diffuses out of the leaf as vapor. Consequently, strong traits associations between leaf hydraulics and stomata have been described in a range of contexts (Sack et al., 2003; Bartlett et al., 2016). In that vein, it is plausible that genes known to alter vascular development via effects on polyamine metabolism (5'-METHYLTHIOADENOSINE NUCLEOSIDASE, MTN1, Waduware-Jayabahu et al., 2012), glucuronoxylan synthesis (BETA-1,4-XYLOSYLTRANSFERASE, IRX9, Pena et al., 2007) and transcriptional regulation (DEFECTIVELY ORGANIZED TRIBUTARIES 5, DOT5, Petricka et al., 2008) might be associated with variation in g_s thermal traits. Stomata closed more slowly in accessions with lower abundance of DOT5 transcripts at the shoot growing point (DOT5 putative ortholog SOBIC.002G164700 in $t_{initial\ min}$, Supplemental Table S3). This is consistent with DOT5 mutants having lower vein density (Wang et al., 2016), which is typically associated with lower stomatal density (Brodribb and Jordan 2011). This is also consistent with low density stomata tending to be larger with slower movements (Pignon et al., 2021).

Similarly, identification of genes involved in photosynthesis may reflect the tight linkage between A and g_s , which is observed in many plant species and is particularly strong in sorghum

(Leakey et al., 2019). QTL for traits related to A and g_s often overlap, including in sorghum (Ortiz et al., 2017). When compared to other species, sorghum shows exceptional coordination between g_s and A following decreases in $PPFD$, driven by rapid responses in g_s (McAusland et al., 2016). Among diverse sorghum accessions, there is significant covariation between the responses of A and g_s following decreases in $PPFD$, i.e. accessions with more rapid declines in A also have more rapid declines in g_s , and vice-versa (Pignon, 2017). Most notable was the identification of the sorghum RUBISCO ACTIVASE (RCA) by GWAS, TWAS and FCT across 8 different g_s *thermal* traits (Supplemental Table S7). RCA encodes an enzyme that plays a key role in activating Rubisco to perform the key step in photosynthetic CO_2 assimilation (Portis 2003), and which is known to limit the rate of photosynthetic induction after an increase in $PPFD$ (Percy 1990). One notable component of the results was significantly lower g_s under high light in sorghum accessions with greater RCA transcript abundance in developing leaf tissues (RCA putative ortholog SOBIC.005G231500 in g_s *light*, Supplemental Table S3). This would be consistent with a general syndrome of high water use efficiency combining low steady-state g_s and fast stomatal movements (Lawson and Blatt 2014; Leakey et al., 2019). Along with a number of the results described above, these findings open the possibility that phenotyping only stomatal closure may have facilitated identification of associations between genotype or gene expression and both stomatal opening and closing, as a result of the two aspects of stomatal movement being so tightly linked. If functional validation of candidate genes supports that notion, then considerable time can be saved when collecting phenotypic data.

Conclusion

This study demonstrates how high-throughput phenotyping by thermal imaging can be used to assess genetic variation in stomatal closure after a decrease in $PPFD$ at a scale suitable for association mapping. Integrated GWAS/TWAS and FCT was then applied to identify a set of candidate genes, which were enriched in putative orthologs of Arabidopsis, maize and rice genes involved in stomatal opening/closing, epidermal patterning, leaf development and photosynthesis. This is important proof of concept for methods to break the phenotyping bottleneck for a trait that is important to plant productivity and sustainability but has until now been intractable as a target for study by quantitative genetics. The method described here could also be applied to other species from a variety of plant functional types or grown in different

522 environments to assess G×E of stomatal traits. In addition, the study provides knowledge of trait
523 variation and underlying candidate genes in an important C₄ model crop, which is notable for the
524 speed of its stomatal opening/closing. This lays the foundation for future studies to establish
525 gene function and potentially improve crop performance.

526

527

Materials and methods

Physiology measurements

Plant material and growing conditions

A random subset of 659 accessions was selected from the biomass sorghum (*Sorghum bicolor*) diversity panel at the University of Illinois at Urbana-Champaign, as previously described (Valluru et al., 2019). Accession names are provided in Supplemental Table S8. Plants were grown from seed in flats (3x6 sets of 281 mL inserts) containing a peat/bark/perlite-based growing medium (Metro-Mix 900; Sun Gro Horticulture, Agawam, MA, USA) and supplemented with 1 mL slow release 13-13-13 fertilizer (Osmocote Classic, Everris NA, Inc., Dublin, OH, USA). One accession, PI147837, was included in each flat to identify spatial and temporal variation in measurements. Three seeds/insert were planted, then thinned to 1 seedling/insert. Flats were watered regularly to field capacity and grown in a greenhouse maintained at 27 °C day/25 °C night, with supplemental lighting to ensure minimum light intensity of 90 W m⁻² during a 13 h day. n=3-4 plants were assessed per accession.

Experimental conditions and leaf temperature measurement

Once the fourth leaf had fully expanded, as evidenced by ligule emergence, plants were transferred to a growth cabinet overnight (Model PCG20, Conviron, Winnipeg, MB R3H 0R9, Canada). Cabinets were maintained at 14 h/10 h day/night cycle under 1200 $\mu\text{mol photons m}^{-2} \text{s}^{-1}$ PPFD, 30 °C daytime/25 °C nighttime temperature, and 75% RH. On the day of measurement, the fourth leaf of each plant was laid flat across a frame to standardize leaf angle and incident light interception (Supplemental Fig. S13). This presented a 4 cm length of the mid-leaf for measurement. Leaves were not detached from plants. Dry and wet reference materials were prepared as in (McAusland et al., 2013) to correct for the effects of net isothermal radiation and VPD, respectively (Guilioni et al., 2008). A thin coating of petroleum jelly was applied over 1 cm of abaxial and adaxial sides of leaves, providing a dry reference unique to each leaf. Two sections of filter paper, moistened by a water reservoir, were used as a wet reference.

Flats of 18 plants were transferred to a second growth cabinet with conditions identical to the first cabinet, except that light was provided by a 20 x 20 cm LED panel providing equal-parts blue, red and green light, with a combined incident photon flux of 750 $\mu\text{mol m}^{-2} \text{s}^{-1}$ at the leaf

level (LED Light Source SL 3500, Photon Systems Instruments, Brno, Czech Republic). An infrared camera (Thermo Gear Model G100, Nippon Avionics CO., Ltd., Tokyo, Japan) was placed 0.5 m above the leaves without obstructing the light source. Incident photon flux was maintained at $750 \mu\text{mol m}^{-2} \text{s}^{-1}$ for 40 minutes, and then reduced by 90% for an additional 60 minutes. Images were recorded every 6 seconds, with emissivity=0.95 (Jones et al., 2002). The cabinet's *PPFD* sensor was used to evaluate spatial heterogeneity of incident photon flux, which was contained to $\pm 6\%$ variation across the measured area.

Image analysis and stomatal conductance estimation

Analysis of thermal images was performed in ImageJ (ImageJ1.51j8, NIH, USA). Sections of leaf and reference materials of each image were hand-selected to derive profiles of temperature vs. experimental time. Leaf and reference temperatures were used to calculate $g_{s \text{ thermal}}$:

$$g_{s \text{ thermal}} = (T_{\text{dry}} - T_{\text{leaf}})/(T_{\text{leaf}} - T_{\text{wet}}) \quad (1)$$

where T_{leaf} , T_{dry} , and T_{wet} are temperatures of the leaf, dry and wet references, respectively. $g_{s \text{ thermal}}$ is theoretically proportional to g_s given constant environmental conditions (Jones, 1999; Jones et al., 2002; Grant et al., 2006; Guilioni et al., 2008; McAusland et al., 2013). Air RH and temperature were controlled by the growth cabinet and assumed constant across all leaf and reference surfaces. Since the cabinet was designed to deliver a uniform airflow, and replicate plantings were randomly positioned to avoid systematic spatial variation, boundary layer conductance was also assumed constant. Differences in $g_{s \text{ thermal}}$ between leaves and over time were therefore attributed to g_s .

Analysis of $g_{s \text{ thermal}}$ profiles

Several traits were derived from profiles of $g_{s \text{ thermal}}$ vs. experimental time: $g_{s \text{ light}}$, $g_{s \text{ shade}}$, $g_{s \Sigma \text{ shade}}$, $g_{s \text{ initial min}}$, $g_{s \text{ oscillation max}}$, $t_{\text{initial min}}$, V_{initial} , and $V_{\text{oscillation}}$. A graphical description of these traits is given in Fig. 1. After the decrease in *PPFD*, $g_{s \text{ thermal}}$ declined as stomata closed, often followed by an oscillation in $g_{s \text{ thermal}}$ as stomata re-opened and then closed again. $g_{s \text{ light}}$ and $g_{s \text{ shade}}$ were the average of $g_{s \text{ thermal}}$ from $t=-5$ to 0, and from $t=52$ to 60 minutes, respectively. These gave steady-state $g_{s \text{ thermal}}$ at *PPFD* of 750 and $75 \mu\text{mol m}^{-2} \text{s}^{-1}$, respectively. $g_{s \Sigma \text{ shade}}$ was the area beneath the curve following the *PPFD* change, i.e. from $t=0$ to 60 minutes. $g_{s \text{ initial min}}$ was the

minimum of $g_{s\text{ thermal}}$ reached immediately after the decrease in $PPFD$. $g_{s\text{ oscillation max}}$ was the maximum of $g_{s\text{ thermal}}$ reached during the stomatal re-opening phase. The time at which $g_{s\text{ thermal}}$ reached 110% of $g_{s\text{ initial min}}$ was recorded as $t_{\text{initial min}}$. The amplitude of the overall change in $g_{s\text{ thermal}}$ from high to low $PPFD$ was $(g_{s\text{ light}} - g_{s\text{ shade}})$, and the amplitude of oscillation in $g_{s\text{ thermal}}$ at low $PPFD$ was $(g_{s\text{ oscillation max}} - g_{s\text{ initial min}})$.

V_{initial} was derived from non-linear regression (PROC NLIN, SAS v9.4; SAS Institute, Cary, NC, USA) as the exponential rate of decline of $g_{s\text{ thermal}}$ from $t = -0.1$ minutes to $t = t_{\text{initial min}}$:

$$g_{s\text{ thermal}} = a + b * e^{(V_{\text{initial}} * \text{time})} \quad (2)$$

here b and a give estimates of $g_{s\text{ thermal}}$ at $t = -0.1$ minutes and $t = t_{\text{initial min}}$, respectively, and a more negative V_{initial} indicates a more rapid decline in $g_{s\text{ thermal}}$. $V_{\text{oscillation}}$ was derived from linear regression (PROC GLM, SAS v9.4) as the linear slope of $g_{s\text{ thermal}}$ vs. time during stomatal re-opening at low $PPFD$. A more positive $V_{\text{oscillation}}$ indicates a more rapid stomatal re-opening.

Validation of $g_{s\text{ thermal}}$ with gas-exchange measurements

Validation of $g_{s\text{ thermal}}$ as a proxy for g_s was obtained on a subset of 64 plants. After $g_{s\text{ thermal}}$ measurements were completed, plants were placed back in the first growth cabinet. The leaf section previously used for $g_{s\text{ thermal}}$ measurements was placed in the cuvette of a portable gas-exchange system incorporating infra-red CO_2 and water vapor analyzers (LI-COR 6400; LI-COR, Inc., Lincoln, NE USA). Incident $PPFD$ was set to $750 \mu\text{mol m}^{-2} \text{s}^{-1}$, $[\text{CO}_2]$ to 400 ppm, and leaf-to-air water vapor pressure deficit maintained <2 kPa. $PPFD$ was 10% blue and 90% red light provided by integrated red and blue LEDs. The $g_{s\text{ thermal}}$ measurement protocol was replicated, i.e. initial $PPFD$ was maintained for 40 minutes, then reduced by 90% for an additional 60 minutes, with g_s logged every 5 seconds (von Caemmerer and Farquhar, 1981). Pearson's correlation (r) at $p=0.05$ threshold, along with Spearman's rank-order correlation (ρ) were tested between equivalent stomatal conductance traits derived from $g_{s\text{ thermal}}$ and g_s using R 3.6.1 (R Core Team, 2017).

When comparing $g_{s\text{ thermal}}$ measurements to this validation data, an anomalous spike in $g_{s\text{ thermal}}$, reaching up to twice the steady-state high- $PPFD$ $g_{s\text{ thermal}}$, was consistently recorded from $t=0$ to 0.9 minutes (Fig. 1). This was likely due to the different radiative properties of the white

wet reference and the green leaf and dry reference. Therefore, $g_{s\text{ thermal}}$ measurements from $t=0$ to 0.9 minutes were discarded.

Model development for best linear unbiased predictors (BLUPs)

A linear mixed model was used to account for spatial and temporal variation using the ASReml-R package (Butler et al., 2009). The best linear unbiased predictors (BLUPs) were obtained for all accessions and traits and were used for subsequent analysis (Supplemental Table S8). The most appropriate model for each trait was chosen in two steps. First, fixed effects with a Wald statistics p -value > 0.05 were excluded from the model. Subsequently, the Akaike information criterion (AIC) was used to select random effects variables and residual variance-covariance structures for each trait. The full model was:

$$y = X\beta + Z_f f + Z_l l + Z_g g + \xi \quad (3)$$

where y is the vector of phenotypes, β is a vector of fixed effects including the intercept, a blocking effect, and a cubic smoothing splines terms for leaf position and time of measurement, with design matrix X . Here the block term refers to three discrete periods throughout the experiment where the LED light had to be repaired and repositioned within the measurement cabinet. The vector f is the vector of random effects of “flat” within block with $f \sim MVN(0, \sigma_{f/r}^2 I_{f/r})$ and design matrix Z_f . Here the term “flat” refers to a sequential flat number to account for temporal variation between measured flats of plants. The vector l is the vector of random effects of the interaction between row leaf position and column leaf position with $l \sim MVN(0, \sigma_l^2 I_l)$ and design matrix Z_l . The vector g is the vector of random genotypic effects of accessions with $g \sim MVN(0, \sigma_g^2 I_g)$ and design matrix Z_g and ξ is the vector of residuals with distribution $\xi \sim MVN(0, R \otimes I_{f/r} \oplus I_r)$. The matrix $R = \sigma_\xi^2 [AR1 \otimes AR1]$ represents the Kronecker product of first-order autoregressive processes across row and column plant positioning within a flat, respectively, and σ_ξ^2 is the spatial residual variance. The matrices $I_{f/r}$, I_g , I_l and I_r are the identity matrices of the same dimensions as “flat” within block, genotypic effects, row leaf position and column leaf position interaction effect, and block, respectively. Outliers were removed following method 2 of (Bernal-Vasquez et al., 2016), and the Box-Cox power transformation was used on traits with non-normal residuals.

BLUPs were obtained for all accessions and each trait and added to the grand mean for GWAS and TWAS. Genetic and residual variances estimated from the null GWAS model were used to calculate genomic heritability (h^2) as the ratio of genetic variance over phenotypic variance (de los Campos et al., 2015). Phenotypic correlations between all traits were tested using Pearson's correlation (r) at $p=0.05$ threshold using `cor.mtest()` function in package `corrplot` (Wei and Simko, 2017).

Genomic data collection for GWAS and TWAS

Genotypic data

Genotyping was performed as previously reported (dos Santos et al., 2020). Briefly, DNA from dark-grown etiolated seedling tissue was extracted and placed in 96-well plates following CTAB protocol (Doyle and Doyle, 1987). The genotyping was done using two pairs of restriction enzymes, PstI-HF/HinP1I and PstI-HF/BfaI (New England Biolabs, Ipswich, MA, USA) with the genotyping-by-sequencing (GBS) protocol (Elshire et al., 2011; Morris et al., 2013). Tag alignment was done with Bowtie2 (Langmead and Salzberg, 2012) using the *Sorghum bicolor* genome v3.1 (www.phytozome.jgi.doe.gov). SNPs were identified using the TASSEL3 GBS pipeline (Glaubitz et al., 2014). Reads that did not perfectly match a barcode and restriction site were discarded. After barcode trimming, all unique 64 bp sequences present >9 times in the dataset and that mapped uniquely to the sorghum genome were selected as "master tags." These were compared to tags in each individual at each genomic address to identify SNPs. SNPs with >95% missing data or minor allele frequency (MAF)<5% were discarded.

A HapMap of 239 whole-genome-resequenced sorghum accessions containing 5.5M biallelic phased SNPs with MAF>0.01 (Valluru et al., 2019), was used as a reference panel to impute the GBS data. GBS markers were filtered to only consider markers that were also present in the HapMap. Beagle 4.1 (Browning and Browning, 2016) was used under GT mode with Ne set to 150,000, window=60,000 SNPs, and overlap=4,000 SNPs. After imputation, markers with $AR2 < 0.3$ were removed, resulting in 2,457,023 SNPs. LD pruning using PLINK (Chang et al., 2015) eliminated markers in high LD ($r^2 > 0.9$) within 50kb windows. The final dataset consisted of 422,897 SNPs.

Gene expression data

113 sorghum accessions were grown for 3'RNAseq measurement. Environmental conditions were: 12 h/12 h day/night cycle under $500 \mu\text{mol m}^{-2} \text{s}^{-1}$ PPFD, 25 °C daytime/23 °C nighttime temperature, and 75% RH. 2 cm of shoot and leaf tissues were sampled at 3rd leaf stage. Samples were processed according to (Kremling et al., 2019). Briefly, RNA was extracted using TRIzol (Invitrogen) with Direct-zol columns (Zymo Research), and 3' RNA-seq libraries were prepared robotically from 500 ng total RNA in 96-well plates on an NXp liquid handler (Beckman Coulter) using QuantSeq FWD kits (Lexogen) according to the manufacturer's instructions. Libraries were pooled to 96-plex and sequenced with 90 nucleotide single-end reads using Illumina TruSeq primers on an Illumina NextSeq 500 with v2 chemistry at the Cornell University Sequencing facility.

The first 12 bp and Illumina Truseq adapter remnants were removed from each read using Trimmomatic version 0.32, following kit marker instructions. The splice-aware STAR aligner v.2.4.2a was used to align reads against the sorghum v3.1.1 reference genome annotations, allowing a read to map in at most 10 locations (-outFilterMultimapNmax 10) with at most 4% mismatches (-outFilterMismatchNoverLmax 0.04), while filtering out non-canonical intron motifs (-outFilterIntronMotifs RemoveNoncanonicalUnannotated). Default settings from STAR v.2.4.2a aligner were used to obtain gene-level counts (--quantModel GeneCounts) from the resulting BAM files.

GWAS, TWAS and FCT

Traits went through an additional normal quantile transformation, then single and multi-trait associations were performed as in (Zhou and Stephens, 2014). Two groups of multi-trait models were considered: G1) traits describing the speed of change in g_s thermal after a decrease in PPFD (V_{initial} , $t_{\text{initial min}}$), and G2) traits describing overall values of g_s thermal (g_s light, g_s initial min, g_s oscillation max, g_s shade, $g_s \Sigma$ shade). Both groups of traits went through a step of multivariate outlier removal (Filzmoser et al., 2005) performed before running GWAS and TWAS.

GEMMA (Zhou and Stephens, 2012) was used for single and multivariate GWAS (Zhou and Stephens, 2014). Population structure was accounted for by using principal components (PCs) as fixed effects. Based on the Scree plot, 4 PCs obtained from PLINK (Chang et al., 2015)

using the full SNP dataset (i.e. not LD-pruned) were included in all models. Relatedness was controlled for by a kinship matrix obtained from TASSEL 5 (Bradbury et al., 2007) using the default method (Endelman and Jannink, 2012).

TWAS was tested in developing leaf and shoot growing point tissues with genes expressed in at least half of tested plants. Analyses were implemented in R 3.3.3 (R Core Team, 2017) with the *lm* function used for single-trait TWAS and the MANOVA function for multi-trait TWAS. Similar to (Kremling et al., 2019), 29 Peer factors (Stegle et al., 2010) and five multidimensional scaling factors were used as covariates. The effect estimate for genes from TWAS was used to determine if there was a positive or negative relationship between transcript abundance and trait variation.

An ensemble approach combining GWAS and TWAS results was performed using the Fisher's combined test (FCT) (Kremling et al., 2019). Briefly, to integrate both the results from GWAS and TWAS, each SNP in the top 10% of GWAS analysis was assigned to the nearest gene. The *p*-values of genes not tested in the TWAS (genes expressed in less than half of tested plants) were set to one. The GWAS and TWAS *p*-values for each gene were combined using Fisher's combined test in *metap* package in R, producing Fisher's combined *p*-values.

Candidate gene analysis

Results of GWAS, TWAS and FCT were used to identify potential candidate genes driving variation in traits. A threshold set at the 0.1% lowest *p*-values was used to identify candidates for each SNP-trait association, i.e., 423 marker associations per trait. This threshold was chosen to focus the analysis on a minimum number of large-effect variants and to limit the number of false positives. PLINK (Chang et al., 2015) was used to calculate LD blocks with option `--blocks` and a window of 200 kb and default values for D-prime's confidence interval (0.7;0.98) (Supplemental Table S1). Genes within these LD blocks were compiled from the Phytozome database for *Sorghum bicolor* v3.1.1 (Goodstein et al., 2012). Similarly, the top 1% most strongly associated genes from TWAS and FCT were ascertained for each trait and tissue. Genes were selected for further analysis if they were identified by more than one test of phenotype-genotype associations, i.e. they overlapped the top hit for several analyses/tissues (e.g. overlapping top hits for both GWAS and TWAS leaf). The Arabidopsis (*Arabidopsis*

thaliana) putative orthologs of these genes were collected with INPARANOID (Remm et al., 2001) and used for GO term enrichment analysis in biological function (GO Ontology database DOI: 10.5281/zenodo.4081749 Released 2020-10-09) (Ashburner et al., 2000; Carbon et al., 2019; Mi et al., 2019). PANTHER overrepresentation test was used with Fisher's test and FDR-adjusted *p*-values, with significance declared at $\alpha < 0.05$. GO biological processes significantly and >2.5-fold enriched were further considered, and the genes contained within these GO categories were considered the strongest candidates to underlie variation in stomatal conductance traits.

Accession Numbers

Accession numbers for the top candidate genes are in Supplemental Table S5.

Supplemental Data

Supplemental Table S1: Linkage disequilibrium (LD) blocks containing the top 0.1% SNPs from GWAS.

Supplemental Table S2: Top 0.1% strongest GWAS results for each trait, including SNP chromosome and position, marker R^2 and minor allele effect size.

Supplemental Table S3: TWAS results from each tissue and trait, including chromosome position, R^2 , and predicted direction of change (+ or -) in phenotype with increased gene expression, for each gene.

Supplemental Table S4: FCT results from each tissue and trait, including the GWAS and TWAS p -values taken from Supplemental Tables S2-3 and used to calculate an FCT p -value for each gene.

Supplemental Table S5: Summary of genes appearing in the top results for GWAS, TWAS leaf, TWAS shoot, FCT leaf and FCT shoot.

Supplemental Table S6: GO enrichment analysis of Arabidopsis putative orthologs of genes overlapping top hits for multiple analyses/tissues.

Supplemental Table S7: Summary of the most promising candidate genes, selected because they belong to a GO biological process category significantly enriched by >2.5-fold among the subset of genes overlapping the top results for GWAS, TWAS leaf, TWAS shoot, FCT leaf, and/or FCT shoot.

Supplemental Table S8: BLUPs of all traits for all accessions.

Supplemental Table S9: Full GWAS results for each trait.

Supplemental Figure S1: Pearson's correlation coefficients (r , top right panels), pairwise correlation scatterplots (bottom left panels) and density plots (diagonal panels) for BLUPs of stomatal traits. Data are the same as in Figure 5.

Supplemental Figure S2: GWAS, TWAS and FCT results for $g_{s \text{ light}}$. A: Upset plot showing the number of overlapping genes between the top hits in GWAS, TWAS leaf, TWAS shoot, FCT leaf, and/or FCT shoot. B: Manhattan plots of GWAS, TWAS and FCT results.

Supplemental Figure S3: GWAS, TWAS and FCT results for $g_{s \text{ shade}}$. A: Upset plot showing the number of overlapping genes between the top hits in GWAS, TWAS leaf, TWAS shoot, FCT leaf, and/or FCT shoot. B: Manhattan plots of GWAS, TWAS and FCT results.

Supplemental Figure S4: GWAS, TWAS and FCT results for $g_{s \text{ oscillation max}}$. A: Upset plot showing the number of overlapping genes between the top hits in GWAS, TWAS leaf, TWAS shoot, FCT leaf, and/or FCT shoot. B: Manhattan plots of GWAS, TWAS and FCT results.

Supplemental Figure S5: GWAS, TWAS and FCT results for $g_{s \text{ initial min}}$. A: Upset plot showing the number of overlapping genes between the top hits in GWAS, TWAS leaf, TWAS shoot, FCT leaf, and/or FCT shoot. B: Manhattan plots of GWAS, TWAS and FCT results.

Supplemental Figure S6: GWAS, TWAS and FCT results for $g_{s \Sigma \text{ shade}}$. A: Upset plot showing the number of overlapping genes between the top hits in GWAS, TWAS leaf, TWAS shoot, FCT leaf, and/or FCT shoot. B: Manhattan plots of GWAS, TWAS and FCT results.

Supplemental Figure S7: GWAS, TWAS and FCT results for $g_{s \text{ light}} - g_{s \text{ shade}}$. A: Upset plot showing the number of overlapping genes between the top hits in GWAS, TWAS leaf, TWAS shoot, FCT leaf, and/or FCT shoot. B: Manhattan plots of GWAS, TWAS and FCT results.

Supplemental Figure S8: GWAS, TWAS and FCT results for $t_{\text{initial min}}$. A: Upset plot showing the number of overlapping genes between the top hits in GWAS, TWAS leaf, TWAS shoot, FCT leaf, and/or FCT shoot. B: Manhattan plots of GWAS, TWAS and FCT results.

Supplemental Figure S9: GWAS, TWAS and FCT results for $V_{\text{oscillation}}$. A: Upset plot showing the number of overlapping genes between the top hits in GWAS, TWAS leaf, TWAS shoot, FCT leaf, and/or FCT shoot. B: Manhattan plots of GWAS, TWAS and FCT results.

789 Supplemental Figure S10: GWAS, TWAS and FCT results for $g_{s\ oscillation\ max} - g_{s\ oscillation\ min}$. A:
790 Upset plot showing the number of overlapping genes between the top hits in GWAS, TWAS
791 leaf, TWAS shoot, FCT leaf, and/or FCT shoot. B: Manhattan plots of GWAS, TWAS and FCT
792 results.

793 Supplemental Figure S11: GWAS, TWAS and FCT results for G2. A: Upset plot showing the
794 number of overlapping genes between the top hits in GWAS, TWAS leaf, TWAS shoot, FCT
795 leaf, and/or FCT shoot. B: Manhattan plots of GWAS, TWAS and FCT results.

796 Supplemental Figure S12: GWAS, TWAS and FCT results for G1. A: Upset plot showing the
797 number of overlapping genes between the top hits in GWAS, TWAS leaf, TWAS shoot, FCT
798 leaf, and/or FCT shoot. B: Manhattan plots of GWAS, TWAS and FCT results.

799 Supplemental Figure S13: Photograph (right) and corresponding thermal image (left) of
800 experimental setup.

801 Supplemental data: Full reference list from literature review of genes in Supplemental Table S7.

802 Tables

803 Table 1: Descriptive statistics of stomatal conductance traits across 659 accessions of sorghum. h^2 is genomic heritability. $t_{initial\ min}$ is in
804 minutes, all other traits are dimensionless. Graphical description of these traits is given in Fig. 1.

Trait	Description	Mean	SD	Min	Max	h^2
$g_{s\ light}$	Steady-state $g_{s\ thermal}$ at high <i>PPFD</i>	0.58	0.08	0.31	0.89	0.31
$g_{s\ shade}$	Steady-state $g_{s\ thermal}$ at low <i>PPFD</i>	0.17	0.07	0.05	0.49	0.70
$(g_{s\ light} - g_{s\ shade})$	Amplitude of overall decline in $g_{s\ thermal}$ from high to low <i>PPFD</i>	0.41	0.08	0.11	0.66	0.31
$g_{s\ initial\ min}$	Minimum $g_{s\ thermal}$ reached after the <i>PPFD</i> decrease	0.05	0.04	-0.03	0.24	0.71
$g_{s\ oscillation\ max}$	Maximum $g_{s\ thermal}$ reached as stomata re-opened at low <i>PPFD</i>	0.20	0.07	0.08	0.53	0.67
$(g_{s\ oscillation\ max} - g_{s\ initial\ min})$	Amplitude of oscillation of $g_{s\ thermal}$ at low <i>PPFD</i>	0.15	0.05	0.05	0.43	0.49
$t_{initial\ min}$	Time for $g_{s\ thermal}$ to reach 110% of $g_{s\ initial\ min}$	5.2	1.6	1.8	13.4	0.68
$g_s \Sigma\ shade$	Area beneath the $g_{s\ thermal}$ curve following the <i>PPFD</i> decrease	84	32	28	231	0.72
$V_{initial}$	Exponential rate of decline in $g_{s\ thermal}$ after the <i>PPFD</i> decrease	-0.89	0.27	-2.23	-0.08	0.67
$V_{oscillation}$	Linear rate of increase in $g_{s\ thermal}$ as stomata re-opened at low <i>PPFD</i>	0.0052	0.0028	0.0006	0.022	0.24

805

806

807 Table 2: N. of genes overlapping the top results of GWAS, TWAS and/or FCT in multiple traits.

N. of overlapping traits	N. of genes
1	4575
2	1463
3	689
4	281
5	150
6	97
7	38
8	11
9	6
10	1

808

809

810

811

812 Figure legends

813 Figure 1: Schematic of $g_{s\text{ thermal}}$ analysis method, where $g_{s\text{ thermal}}$ is a proxy for stomatal conductance to water vapor (g_s) that is derived
 814 from thermal imaging. Each response was measured on a single leaf of sorghum, exposed to $PPFD=750\text{ }\mu\text{mol m}^{-2}\text{ s}^{-1}$ for 40 minutes.
 815 At $t=0$, indicated by an arrow, $PPFD$ was reduced by 90%. Black circles show $g_{s\text{ thermal}}$. Crosses show measurements from $t=0$ to $t=0.9$
 816 minutes which were removed because they consistently showed an anomalous spike. $g_{s\text{ light}}$, the steady-state high- $PPFD$ value of g_s
 817 $thermal$, was the mean $g_{s\text{ thermal}}$ from $t=-5$ to 0 minutes (red circle). $g_{s\text{ shade}}$, the steady-state low- $PPFD$ value of $g_{s\text{ thermal}}$, was the mean g_s
 818 $thermal$ from $t=52$ to 60 minutes (blue circle). $g_{s\text{ } \Sigma\text{ shade}}$ was the area under the curve from $t=0$ to 60 minutes. $g_{s\text{ initial min}}$ was the minimum
 819 of $g_{s\text{ thermal}}$ reached immediately after the decrease in $PPFD$ (orange circle). $g_{s\text{ oscillation max}}$ was the maximum of $g_{s\text{ thermal}}$ reached during
 820 stomatal re-opening at low $PPFD$ (pink circle). The time at which $g_{s\text{ thermal}}$ reached 110% of $g_{s\text{ initial min}}$ was recorded as $t_{\text{initial min}}$ (dotted
 821 orange line). V_{initial} , the initial rate of decline in $g_{s\text{ thermal}}$ after the decrease in $PPFD$, was the exponential rate of decline of $g_{s\text{ thermal}}$ $t=-$
 822 0.1 minutes to $t=t_{\text{initial min}}$ (solid green line). $V_{\text{oscillation}}$ was the linear rate of increase in $g_{s\text{ thermal}}$ during stomatal reopening at low $PPFD$
 823 (dashed green line).

824 Figure 2: Representative responses of $g_{s\text{ thermal}}$ and g_s to a 90% drop in $PPFD$ for two accessions: PI455257 and PI525728. $g_{s\text{ thermal}}$ was
 825 measured from thermal imaging as a proxy for g_s . Each $g_{s\text{ thermal}}$ response curve was measured on a single leaf, acclimated to
 826 $PPFD=750\text{ }\mu\text{mol m}^{-2}\text{ s}^{-1}$ for 40 minutes, then $PPFD$ was reduced by 90% for 60 minutes at $t=0$, indicated by an arrow. On a subset of
 827 plants, including the two shown here, the protocol was immediately repeated to measure g_s using gas exchange.

828 Figure 3: Correlation scatterplots between stomatal conductance traits derived from $g_{s\text{ thermal}}$ measurements and their counterparts
 829 derived from g_s measurements. A: $g_{s\text{ light}}$, B: $g_{s\text{ shade}}$, C: $g_{s\text{ light}} - g_{s\text{ shade}}$, D: $g_{s\text{ initial min}}$, E: $g_{s\text{ oscillation max}}$, F: $g_{s\text{ oscillation max}} - g_{s\text{ initial min}}$, G: $g_{s\text{ } \Sigma\text{ shade}}$, H: $t_{\text{initial min}}$, I: V_{initial} , J: $V_{\text{oscillation}}$. Data are for a subset of plants that were first imaged using a thermal camera to obtain $g_{s\text{ thermal}}$,
 830 then immediately measured with gas exchange to obtain g_s . Pearson's r and the associated p -value, along with Spearman's rank-order
 831 ρ , are also given.

833 Figure 4: Representative responses of $g_{s\text{ thermal}}$ to a 90% decrease in $PPFD$ in six accessions, selected to highlight the diverse stomatal
 834 responses to decreasing $PPFD$ measured in the sorghum diversity panel. A: PI552851, B: PI267653, C: NSL50717, D: PI660605, E:
 835 PI329646, F: PI660630. Different symbols and shades of gray show distinct replicate plants for each accession. Each $g_{s\text{ thermal}}$ response
 836 curve was measured on a single leaf, acclimated to $PPFD=750\text{ }\mu\text{mol m}^{-2}\text{ s}^{-1}$ for 40 minutes, then $PPFD$ was reduced by 90% for 60
 837 minutes at $t=0$, indicated by an arrow. Values in the table are the mean ($n=3-4$ plants) of stomatal conductance traits for each
 838 accession. $t_{\text{initial min}}$ is in minutes, all other traits are dimensionless.

839 Figure 5: Pearson's correlation coefficients (r) between BLUPs of stomatal conductance traits. The size of circles indicates the
 840 strength of correlation, while color indicates whether the pairwise relationship was negative ($r<0$, red) or positive ($r>0$, blue). All
 841 corresponding scatterplots are given in Supplemental Fig. S1.

842 Figure 6: Correlation scatterplots between BLUPs for stomatal conductance traits. A: $g_{s\text{ shade}}$ vs. $g_{s\text{ light}}$, B: $t_{\text{initial min}}$ vs. $g_{s\text{ light}}$, C: V_{initial}
 843 vs. $g_{s\text{ light}}$, D: $V_{\text{oscillation}}$ vs. $g_{s\text{ light}}$. Pearson's r and the associated p -value are also given.

844 Figure 7: GWAS, TWAS and FCT results for $g_{s\text{ light}}$. A: Upset plot showing the number of overlapping genes between the top hits in
 845 GWAS, TWAS leaf, TWAS shoot, FCT leaf, and/or FCT shoot. B: Manhattan plots of GWAS, TWAS and FCT results. Top hits are
 846 highlighted if they correspond to putative orthologs of known Arabidopsis stomatal genes (FMA, POLAR and EPF2, Table 3). Top
 847 hits are also highlighted if they are among the highest confidence genes identified by GWAS, TWAS, FCT, and subsequent GO
 848 enrichment analysis. (Supplemental Table S7). Equivalent figures for all other traits are in Supplemental Figures S2-12.

849 Figure 8: Results of GO enrichment analysis of higher confidence genes. Bars gives the number of genes included in each of the
 850 categories of GO biological processes that were significantly and >2.5 -fold enriched. Fold-enrichment is shown in the label beneath
 851 each bar. Full GO enrichment analysis results are in Supplemental Table S6.

852

References

- Acevedo-Siaca LG, Coe R, Wang Y, Kromdijk J, Quick WP, Long SP** (2020) Variation in photosynthetic induction between rice accessions and its potential for improving productivity. *New Phytologist*: 12
- Ashburner M, Ball CA, Blake JA, Botstein D, Butler H, Cherry JM, Davis AP, Dolinski K, Dwight SS, Eppig JT, Harris MA, Hill DP, Issel-Tarver L, Kasarskis A, Lewis S, Matese JC, Richardson JE, Ringwald M, Rubin GM, Sherlock G, Gene Ontology C** (2000) Gene Ontology: tool for the unification of biology. *Nature Genetics* **25**: 25-29
- Assmann SM, Jegla T** (2016) Guard cell sensory systems: recent insights on stomatal responses to light, abscisic acid, and CO₂. *Current Opinion in Plant Biology* **33**: 157-167
- Assmann SM, Shimazaki K** (1999) The multisensory guard cell. Stomatal responses to blue light and abscisic acid. *Plant Physiology* **119**: 809-815
- Ball JT, Woodrow IE, Berry JAB** (1987) A model predicting stomatal conductance and its contribution to the control of photosynthesis under different environmental conditions. *In* J Biggins, ed, *Progress in photosynthesis research*. Springer Netherlands, pp 221-224
- Ballard T, Peak D, Mott K** (2019) Blue and red light effects on stomatal oscillations. *Functional Plant Biology* **46**: 146-151
- Bernal-Vasquez AM, Utz HF, Piepho HP** (2016) Outlier detection methods for generalized lattices: a case study on the transition from ANOVA to REML. *Theoretical and Applied Genetics* **129**: 787-804
- Boyer JS** (1982) Plant productivity and environment. *Science* **218**: 443-448
- Bradbury PJ, Zhang Z, Kroon DE, Casstevens TM, Ramdoss Y, Buckler ES** (2007) TASSEL: software for association mapping of complex traits in diverse samples. *Bioinformatics* **23**: 2633-2635
- Brodribb TJ, Jordan GJ** (2011) Water supply and demand remain balanced during leaf acclimation of *Nothofagus cunninghamii* trees. *New Phytologist* **192**(2): 437-448
- Browning BL, Browning SR** (2016) Genotype Imputation with Millions of Reference Samples. *American Journal of Human Genetics* **98**: 116-126
- Burks PS, Kaiser CM, Hawkins EM, Brown PJ** (2015) Genomewide Association for Sugar Yield in Sweet Sorghum. *Crop Science* **55**: 2138-2148
- Butler DG, Cullis BR, Gilmour AR, Gogel BJ** (2009) ASReml-R reference manual. *The State of Queensland, Department of Primary Industries and Fisheries, Brisbane* .
- Carbon S, Douglass E, Dunn N, Good B, Harris NL, Lewis SE, Mungall CJ, Basu S, Chisholm RL, Dodson RJ, Hartline E, Fey P, Thomas PD, Albou LP, Ebert D, Kesling MJ, Mi H, Muruganujan A, Huang X, Poudel S, Mushayahama T, Hu JC, LaBonte SA, Siegele DA, Antonazzo G, Attrill H, Brown NH, Fexova S, Garapati P, Jones TEM, Marygold SJ, Millburn GH, Rey AJ, Trovisco V, dos**

- Santos G, Emmert DB, Falls K, Zhou P, Goodman JL, Strelets VB, Thurmond J, Courtot M, Osumi-Sutherland D, Parkinson H, Roncaglia P, Acencio ML, Kuiper M, Laegreid A, Logie C, Lovering RC, Huntley RP, Denny P, Campbell NH, Kramarz B, Acquaah V, Ahmad SH, Chen H, Rawson JH, Chibucos MC, Giglio M, Nadendla S, Tauber R, Duesbury MJ, Del-Toro N, Meldal BHM, Perfetto L, Porras P, Orchard S, Shrivastava A, Xie Z, Chang HY, Finn RD, Mitchell AL, Rawlings ND, Richardson L, Sangrador-Vegas A, Blake JA, Christie KR, Dolan ME, Drabkin HJ, Hill DP, Ni L, Sitnikov D, Harris MA, Oliver SG, Rutherford K, Wood V, Hayles J, Bahler J, Lock A, Bolton ER, De Pons J, Dwinell M, Hayman GT, Laulederkind SJF, Shimoyama M, Tutaj M, Wang SJ, D'Eustachio P, Matthews L, Balhoff JP, Aleksander SA, Binkley G, Dunn BL, Cherry JM, Engel SR, Gondwe F, Karra K, MacPherson KA, Miyasato SR, Nash RS, Ng PC, Sheppard TK, Shrivatsav VPA, Simison M, Skrzypek MS, Weng S, Wong ED, Feuermann M, Gaudet P, Bakker E, Berardini TZ, Reiser L, Subramaniam S, Huala E, Arighi C, Auchincloss A, Axelsen K, Argoud-Puy G, Bateman A, Bely B, Blatter MC, Boutet E, Breuza L, Bridge A, Britto R, Bye-A-Jee H, Casals-Casas C, Coudert E, Estreicher A, Famiglietti L, Garmiri P, Georghiou G, Gos A, Gruaz-Gumowski N, Hatton-Ellis E, Hinz U, Hulo C, Ignatchenko A, Jungo F, Keller G, Laiho K, Lemercier P, Lieberherr D, Lussi Y, Mac-Dougall A, Magrane M, Martin MJ, Masson P, Natale DA, Hyka-Nouspikel N, Pedruzzi I, Pichler K, Poux S, Rivoire C, Rodriguez-Lopez M, Sawford T, Speretta E, Shypitsyna A, Stutz A, Sundaram S, Tognolli M, Tyagi N, Warner K, Zaru R, Wu C, Diehl AD, Chan J, Cho J, Gao S, Grove C, Harrison MC, Howe K, Lee R, Mendel J, Muller HM, Raciti D, Van Auken K, Berriman M, Stein L, Sternberg PW, Howe D, Toro S, Westerfield M, Gene Ontology C (2019) The Gene Ontology Resource: 20 years and still GOing strong. *Nucleic Acids Research* **47**: D330-D338
- Casa AM, Pressoir G, Brown PJ, Mitchell SE, Rooney WL, Tuinstra MR, Franks CD, Kresovich S (2008) Community resources and strategies for association mapping in sorghum. *Crop Science* **48**: 30-40
- Chang CC, Chow CC, Tellier L, Vattikuti S, Purcell SM, Lee JJ (2015) Second-generation PLINK: rising to the challenge of larger and richer datasets. *Gigascience* **4**: 16
- de los Campos G, Sorensen D, Gianola D (2015) Genomic Heritability: What Is It? *Plos Genetics* **11**: 21
- De Souza AP, Wang Y, Orr DJ, Carmo-Silva E, Long SP (2020) Photosynthesis across African cassava germplasm is limited by Rubisco and mesophyll conductance at steady state, but by stomatal conductance in fluctuating light. *New Phytologist* **225**: 2498-2512
- Deans RM, Brodribb TJ, Busch FA, Farquhar GD (2019) Plant water-use strategy mediates stomatal effects on the light induction of photosynthesis. *New Phytologist* **222**: 382-395
- DeLucia EH, Chen S, Guan K, Peng B, Li Y, Gomez-Casanovas N, Kantola IB, Bernacchi CJ, Huang Y, Long SP, Ort DR (2019) Are we approaching a water ceiling to maize yields in the United States? *Ecosphere* **10**(6)
- dos Santos JPR, Fernandes SB, McCoy S, Lozano R, Brown PJ, Leakey ADB, Buckler ES, Garcia AAF, Gore MA (2020) Novel Bayesian Networks for Genomic Prediction of Developmental Traits in Biomass Sorghum. *G3-Genes Genomes Genetics* **10**: 769-781

- Dow GJ, Bergmann DC, Berry JA** (2014) An integrated model of stomatal development and leaf physiology. *New Phytologist* **201**: 1218-1226
- Doyle J, Doyle J** (1987) A rapid procedure for DNA purification from small quantities of fresh leaf tissue. . *Phytochemical Bulletin* **19**: 11-15
- Durand M, Brendel O, Bure C, Le Thiec D** (2019) Altered stomatal dynamics induced by changes in irradiance and vapour-pressure deficit under drought: impacts on the whole-plant transpiration efficiency of poplar genotypes. *New Phytologist* **222**: 1789-1802
- Edwards EJ, Osborne CP, Stromberg CAE, Smith SA, Bond WJ, Christin PA, Cousins AB, Duvall MR, Fox DL, Freckleton RP, Ghannoum O, Hartwell J, Huang YS, Janis CM, Keeley JE, Kellogg EA, Knapp AK, Leahey ADB, Nelson DM, Saarela JM, Sage RF, Sala OE, Salamin N, Still CJ, Tipple B, Consortium CG** (2010) The Origins of C₄ Grasslands: Integrating Evolutionary and Ecosystem Science. *Science* **328**: 587-591
- Elshire RJ, Glaubitz JC, Sun Q, Poland JA, Kawamoto K, Buckler ES, Mitchell SE** (2011) A Robust, Simple Genotyping-by-Sequencing (GBS) Approach for High Diversity Species. *Plos One* **6**: 10
- Endelman JB, Jannink JL** (2012) Shrinkage Estimation of the Realized Relationship Matrix. *G3-Genes Genomes Genetics* **2**: 1405-1413
- Fahlgren N, Feldman M, Gehan MA, Wilson MS, Shyu C, Bryant DW, Hill ST, McEntee CJ, Warnasooriya SN, Kumar I, Ficor T, Turnipseed S, Gilbert KB, Brutnell TP, Carrington JC, Mockler TC, Baxter I** (2015) A Versatile Phenotyping System and Analytics Platform Reveals Diverse Temporal Responses to Water Availability in *Setaria*. *Molecular Plant* **8**: 1520-1535
- FAO, IFAD, UNICEF, WFP, WHO** (2018) The State of Food Security and Nutrition in the World 2018. Building climate resilience for food security and nutrition. *In*. FAO, Rome, p 202
- Faralli M, Matthews J, Lawson T** (2019) Exploiting natural variation and genetic manipulation of stomatal conductance for crop improvement. *Current Opinion in Plant Biology* **49**: 1-7
- JF Ferguson, SB Fernandes, B Monier, ND Miller, D Allen, A Dmitrieva, P Schmuker, R Lozano, R Valluru, ES Buckler, MA Gore, PJ Brown, EP Spalding, ADB Leahey** (2021) Machine learning enabled phenotyping for GWAS and TWAS of WUE traits in 869 field-grown sorghum accessions. *Plant Physiology* in press
- Filzmoser P, Garrett RG, Reimann C** (2005) Multivariate outlier detection in exploration geochemistry. *Computers & Geosciences* **31**: 579-587
- Franks PJ, Farquhar GD** (2007) The mechanical diversity of stomata and its significance in gas-exchange control. *Plant Physiology* **143**: 78-87
- Glaubitz JC, Casstevens TM, Lu F, Harriman J, Elshire RJ, Sun Q, Buckler ES** (2014) TASSEL-GBS: A High Capacity Genotyping by Sequencing Analysis Pipeline. *Plos One* **9**: 11

- Goodstein DM, Shu SQ, Howson R, Neupane R, Hayes RD, Fazo J, Mitros T, Dirks W, Hellsten U, Putnam N, Rokhsar DS** (2012) Phytozome: a comparative platform for green plant genomics. *Nucleic Acids Research* **40**: D1178-D1186
- Grant OM, Chaves MM, Jones HG** (2006) Optimizing thermal imaging as a technique for detecting stomatal closure induced by drought stress under greenhouse conditions. *Physiologia Plantarum* **127**: 507-518
- Grant OM, Tronina L, Jones HG, Chaves MM** (2007) Exploring thermal imaging variables for the detection of stress responses in grapevine under different irrigation regimes. *Journal of Experimental Botany* **58**: 815-825
- Guilioni L, Jones HG, Leinonen I, Lhomme JP** (2008) On the relationships between stomatal resistance and leaf temperatures in thermography. *Agricultural and Forest Meteorology* **148**: 1908-1912
- Hadebe ST, Modi AT, Mabhaudhi T** (2017) Drought Tolerance and Water Use of Cereal Crops: A Focus on Sorghum as a Food Security Crop in Sub-Saharan Africa. *Journal of Agronomy and Crop Science* **203**: 177-191
- Hetherington AM, Woodward FI** (2003) The role of stomata in sensing and driving environmental change. *Nature* **424**: 901-908
- Jones HG** (1999) Use of infrared thermometry for estimation of stomatal conductance as a possible aid to irrigation scheduling. *Agricultural and Forest Meteorology* **95**: 139-149
- Jones HG, Stoll M, Santos T, de Sousa C, Chaves MM, Grant OM** (2002) Use of infrared thermography for monitoring stomatal closure in the field: application to grapevine. *Journal of Experimental Botany* **53**: 2249-2260
- Kaiser E, Morales A, Harbinson J** (2018) Fluctuating Light Takes Crop Photosynthesis on a Rollercoaster Ride. *Plant Physiology* **176**: 977-989
- Kaiser E, Morales A, Harbinson J, Kromdijk J, Heuvelink E, Marcelis LFM** (2015) Dynamic photosynthesis in different environmental conditions. *Journal of Experimental Botany* **66**: 2415-2426
- Kaiser H, Kappen L** (2001) Stomatal oscillations at small apertures: indications for a fundamental insufficiency of stomatal feedback-control inherent in the stomatal turgor mechanism. *Journal of Experimental Botany* **52**: 1303-1313
- Kerstiens G** (1996) Cuticular water permeability and its physiological significance. *Journal of Experimental Botany* **47**: 1813-1832
- Koester RP, Nohl BM, Diers BW, Ainsworth EA** (2016) Has photosynthetic capacity increased with 80 years of soybean breeding? An examination of historical soybean cultivars. *Plant Cell and Environment* **39**: 1058-1067
- Kremling KAG, Diepenbrock CH, Gore MA, Buckler ES, Bandillo NB** (2019) Transcriptome-Wide Association Supplements Genome-Wide Association in *Zea mays*. *G3-Genes Genomes Genetics* **9**: 3023-3033
- Langmead B, Salzberg SL** (2012) Fast gapped-read alignment with Bowtie 2. *Nature Methods* **9**: 357-U354
- Lawson T, Blatt MR** (2014) Stomatal Size, Speed, and Responsiveness Impact on Photosynthesis and Water Use Efficiency. *Plant Physiology* **164**: 1556-1570
- Lawson T, Viallet-Chabrand S** (2019) Speedy stomata, photosynthesis and plant water use efficiency. *New Phytologist* **221**: 93-98

974 **Lawson T, von Caemmerer S, Baroli I** (2011) Photosynthesis and Stomatal Behaviour. *In* U Luttge, W Beyschlag, B Budel, D Francis,
975 eds, Progress in Botany 72, Vol 72. Springer-Verlag Berlin, Berlin, pp 265-304

976 **Leakey ADB, Ferguson JN, Pignou CP, Wu A, Jin Z, Hammer GL, Lobell DB** (2019) Water use efficiency as a constraint and target for
977 improving the resilience and productivity of C₃ and C₄ crops. *Annual Review of Plant Biology* **70**: 781-808

978 **Liu HJ, Yan JB** (2019) Crop genome-wide association study: a harvest of biological relevance. *Plant Journal* **97**: 8-18

979 **Lobell DB, Burke MB, Tebaldi C, Mastrandrea MD, Falcon WP, Naylor RL** (2008) Prioritizing climate change adaptation needs for
980 food security in 2030. *Science* **319**: 607-610

981 **Lobell DB, Roberts MJ, Schlenker W, Braun N, Little BB, Rejesus RM, Hammer GL** (2014) Greater Sensitivity to Drought
982 Accompanies Maize Yield Increase in the US Midwest. *Science* **344**: 516-519

983 **McAdam SAM, Brodribb TJ** (2015) The Evolution of Mechanisms Driving the Stomatal Response to Vapor Pressure Deficit. *Plant*
984 *Physiology* **167**: 833-843

985 **McAusland L, Davey PA, Kanwal N, Baker NR, Lawson T** (2013) A novel system for spatial and temporal imaging of intrinsic plant
986 water use efficiency. *Journal of Experimental Botany* **64**: 4993-5007

987 **McAusland L, Violet-Chabrand S, Davey P, Baker NR, Brendel O, Lawson T** (2016) Effects of kinetics of light-induced stomatal
988 responses on photosynthesis and water-use efficiency. *New Phytologist* **211**: 1209-1220

989 **Merlot S, Mustilli AC, Genty B, North H, Lefebvre V, Sotta B, Vavasseur A, Giraudat J** (2002) Use of infrared thermal imaging to
990 isolate Arabidopsis mutants defective in stomatal regulation. *Plant Journal* **30**: 601-609

991 **Mi HY, Muruganujan A, Ebert D, Huang XS, Thomas PD** (2019) PANTHER version 14: more genomes, a new PANTHER GO-slim and
992 improvements in enrichment analysis tools. *Nucleic Acids Research* **47**: D419-D426

993 **Morris GP, Ramu P, Deshpande SP, Hash CT, Shah T, Upadhyaya HD, Riera-Lizarazu O, Brown PJ, Acharya CB, Mitchell SE,**
994 **Harriman J, Glaubitz JC, Buckler ES, Kresovich S** (2013) Population genomic and genome-wide association studies of
995 agroclimatic traits in sorghum. *Proceedings of the National Academy of Sciences of the United States of America* **110**: 453-
996 458

997 **Nunes TDG, Zhang D, Raissig MT** (2020) Form, development and function of grass stomata. *Plant Journal* **101**: 780-799

998 **Ort DR, Long SP** (2014) Limits on Yields in the Corn Belt. *Science* **344**: 483-484

999 **Ortiz D, Hu JY, Fernandez MGS** (2017) Genetic architecture of photosynthesis in Sorghum bicolor under non-stress and cold stress
1000 conditions. *Journal of Experimental Botany* **68**: 4545-4557

1001 **Papanatsiou M, Petersen J, Henderson L, Wang Y, Christie JM, Blatt MR** (2019) Optogenetic manipulation of stomatal kinetics
1002 improves carbon assimilation, water use, and growth. *Science* **363**: 1456-+

1003 **Paterson AH, Bowers JE, Bruggmann R, Dubchak I, Grimwood J, Gundlach H, Haberer G, Hellsten U, Mitros T, Poliakov A, Schmutz**
1004 **J, Spannagl M, Tang HB, Wang XY, Wicker T, Bharti AK, Chapman J, Feltus FA, Gowik U, Grigoriev IV, Lyons E, Maher CA,**

1005 **Martis M, Narechania A, Otilar RP, Penning BW, Salamov AA, Wang Y, Zhang LF, Carpita NC, Freeling M, Gingle AR, Hash**
 1006 **CT, Keller B, Klein P, Kresovich S, McCann MC, Ming R, Peterson DG, Mehboob ur R, Ware D, Westhoff P, Mayer KFX,**
 1007 **Messing J, Rokhsar DS** (2009) The *Sorghum bicolor* genome and the diversification of grasses. *Nature* **457**: 551-556
 1008 **Pearcy RW** (1990) Sunflecks and photosynthesis in plant canopies. *Annual Review of Plant Physiology and Plant Molecular Biology*
 1009 **41**: 421-453
 1010 **Pignou CP** (2017) Strategies to improve C₄ photosynthesis, water and resource-use efficiency under different atmospheres,
 1011 temperatures, and light environments. University of Illinois at Urbana-Champaign, Urbana, Illinois
 1012 **Pignou CP, Leahey ADB, Long SP, Kromdijk J** (2021) Drivers of Natural Variation in Water-Use Efficiency Under Fluctuating Light Are
 1013 Promising Targets for Improvement in Sorghum. *Frontiers in Plant Science* **12**: 13
 1014 **PT Prakash, D Banan, RE Paul, MJ Feldman, D Xie, L Freyfogle, I Baxter, ADB Leahey** (2021) Correlation and co-localization of QTL
 1015 for stomatal density and canopy temperature under drought stress in *Setaria*. *Journal of Experimental Botany* (in press).
 1016 **R Core Team** (2017) R: A language and environment for statistical computing., R Foundation for Statistical Computing, Vienna,
 1017 Australia
 1018 **Ray DK, Mueller ND, West PC, Foley JA** (2013) Yield Trends Are Insufficient to Double Global Crop Production by 2050. *Plos One* **8**: 8
 1019 **Regassa TH, Wortmann CS** (2014) Sweet sorghum as a bioenergy crop: Literature review. *Biomass & Bioenergy* **64**: 348-355
 1020 **Remm M, Storm CEV, Sonnhammer ELL** (2001) Automatic clustering of orthologs and in-paralogs from pairwise species
 1021 comparisons. *Journal of Molecular Biology* **314**: 1041-1052
 1022 **Sagan V, Maimaitijiang M, Sidike P, Eblimit K, Peterson KT, Hartling S, Esposito F, Khanal K, Newcomb M, Pauli D, Ward R, Fritschi**
 1023 **F, Shakoore N, Mockler T** (2019) UAV-Based High Resolution Thermal Imaging for Vegetation Monitoring, and Plant
 1024 Phenotyping Using ICI 8640 P, FLIR Vue Pro R 640, and thermoMap Cameras. *Remote Sensing* **11**
 1025 **Serna L** (2011) Stomatal development in *Arabidopsis* and grasses: differences and commonalities. *International Journal of*
 1026 *Developmental Biology* **55**: 5-10
 1027 **Shimazaki K, Doi M, Assmann SM, Kinoshita T** (2007) Light regulation of stomatal movement. *Annual Review of Plant Biology* **58**:
 1028 219-247
 1029 **Sinclair TR, Tanner CB, Bennett JM** (1984) Water-use efficiency in crop production. *Bioscience* **34**: 36-40
 1030 **Soleh MA, Tanaka Y, Nomoto Y, Iwahashi Y, Nakashima K, Fukuda Y, Long SP, Shiraiwa T** (2016) Factors underlying genotypic
 1031 differences in the induction of photosynthesis in soybean *Glycine max* (L.) Merr. *Plant Cell and Environment* **39**: 685-693
 1032 **Stegle O, Parts L, Durbin R, Winn J** (2010) A Bayesian Framework to Account for Complex Non-Genetic Factors in Gene Expression
 1033 Levels Greatly Increases Power in eQTL Studies. *Plos Computational Biology* **6**: 11
 1034 **Takahashi S, Monda K, Negi J, Konishi F, Ishikawa S, Hashimoto-Sugimoto M, Goto N, Iba K** (2015) Natural Variation in Stomatal
 1035 Responses to Environmental Changes among *Arabidopsis thaliana* Ecotypes. *Plos One* **10**: 13

1036 **Tam V, Patel N, Turcotte M, Bosse Y, Pare G, Meyre D** (2019) Benefits and limitations of genome-wide association studies. *Nature*
1037 *Reviews Genetics* **20**: 467-484

1038 **Valluru R, Gazave EE, Fernandes SB, Ferguson JN, Lozano R, Hirannaiah P, Zuo T, Brown PJ, Leahey ADB, Gore MA, Buckler ES,**
1039 **Bandillo N** (2019) Deleterious Mutation Burden and Its Association with Complex Traits in Sorghum (*Sorghum bicolor*).
1040 *Genetics* **211**: 1075-1087

1041 **Vialet-Chabrand S, Lawson T** (2019) Dynamic leaf energy balance: deriving stomatal conductance from thermal imaging in a dynamic
1042 environment. *Journal of Experimental Botany* **70**: 2839-2855

1043 **Vico G, Manzoni S, Palmroth S, Katul G** (2011) Effects of stomatal delays on the economics of leaf gas exchange under intermittent
1044 light regimes. *New Phytologist* **192**: 640-652

1045 **von Caemmerer S, Farquhar GD** (1981) Some relationships between the biochemistry of photosynthesis and the gas exchange of
1046 leaves. *Planta* **153**: 376-387

1047 **Wang Y, Burgess SJ, de Becker EM, Long SHP** (2020) Photosynthesis in the fleeting shadows: an overlooked opportunity for
1048 increasing crop productivity? *Plant Journal* **101**: 874-884

1049 **Way DA, Pearcy RW** (2012) Sunflecks in trees and forests: from photosynthetic physiology to global change biology. *Tree Physiology*
1050 **32**: 1066-1081

1051 **Wei T, Simko V** (2017) R package "corrplot": Visualization of a Correlation Matrix. *In*,
1052 **Wong SC, Cowan IR, Farquhar GD** (1979) Stomatal conductance correlates with photosynthetic capacity. *Nature* **282**: 424-426

1053 **WWAP** (2015) The United Nations world water development report 2015: Water for a sustainable world. *In*. UNESCO, Paris

1054 **Zhou X, Stephens M** (2012) Genome-wide efficient mixed-model analysis for association studies. *Nature Genetics* **44**: 821-U136

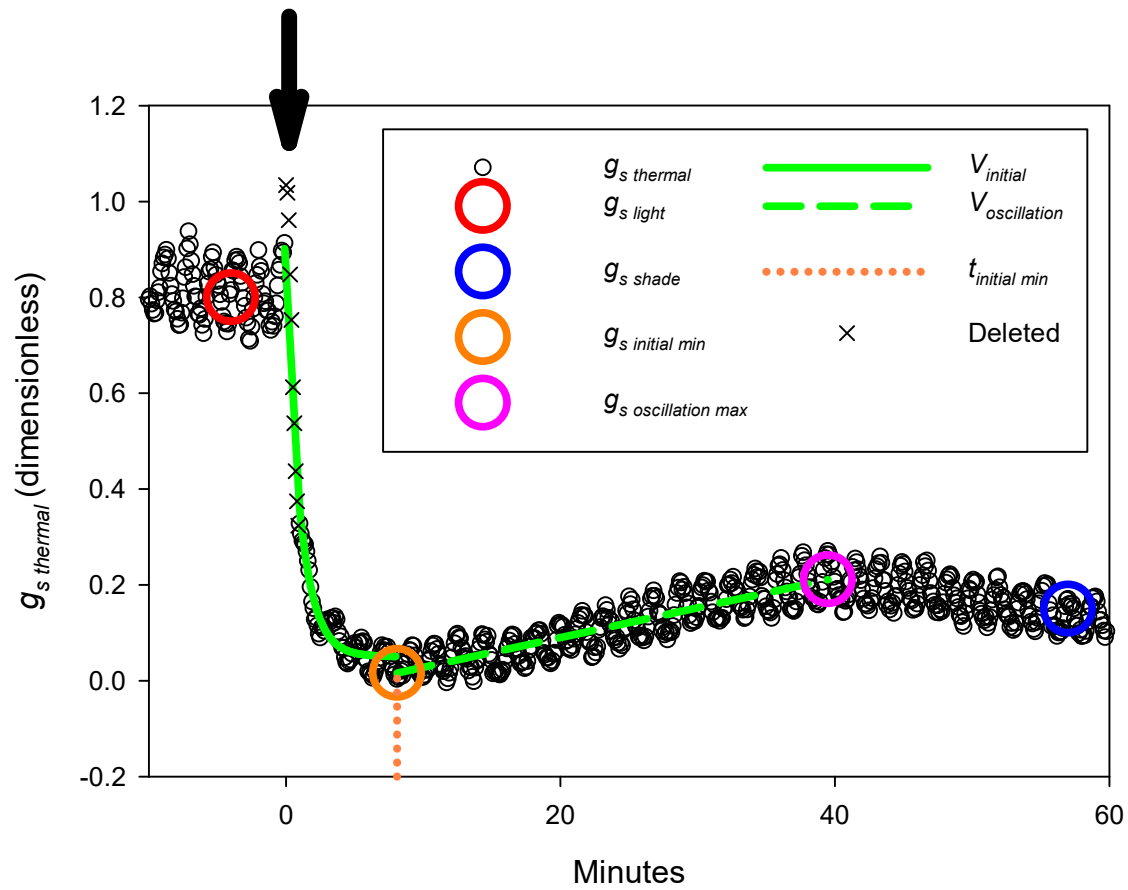
1055 **Zhou X, Stephens M** (2014) Efficient multivariate linear mixed model algorithms for genome-wide association studies. *Nature*
1056 *Methods* **11**: 407-+

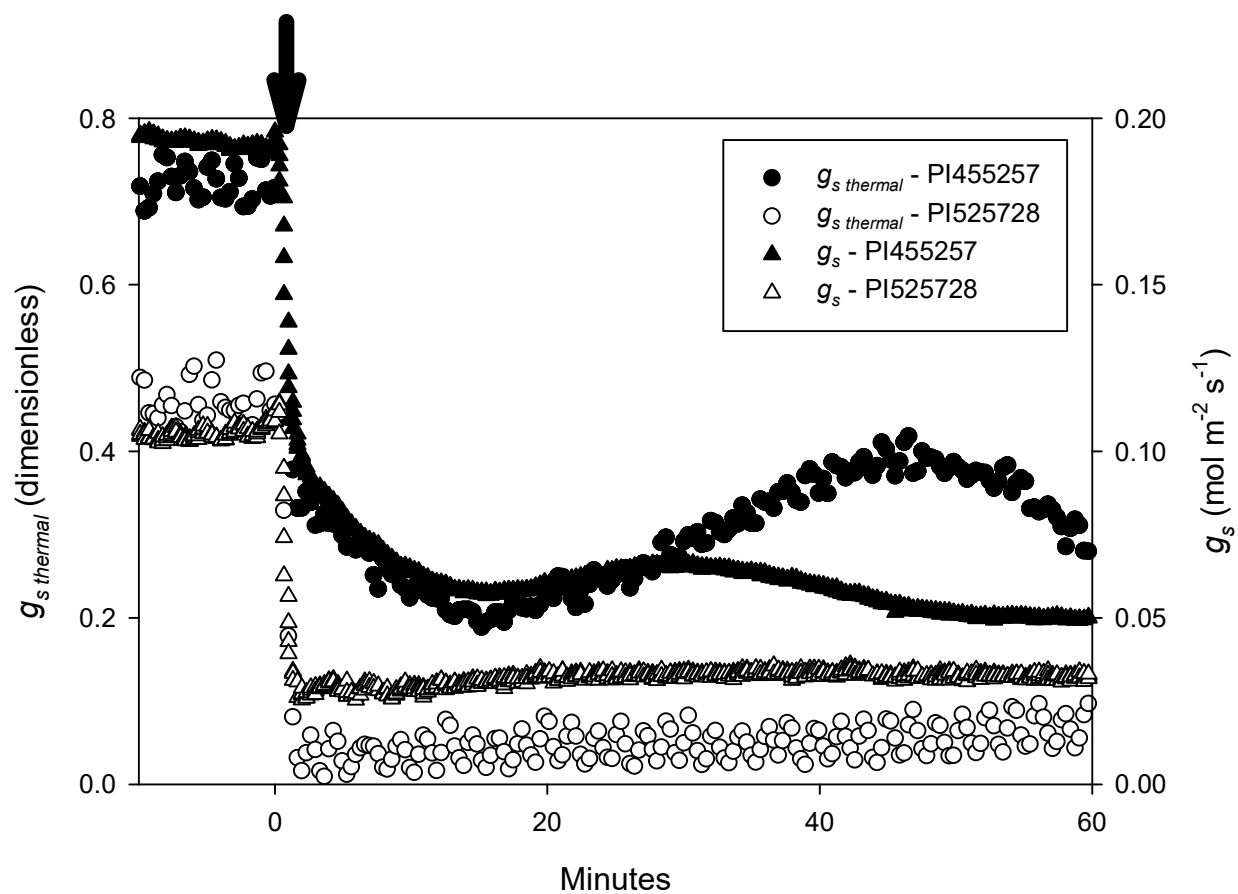
1057 **Zhou XY, Huang XH** (2019) Genome-wide Association Studies in Rice: How to Solve the Low Power Problems? *Molecular Plant* **12**:
1058 10-12

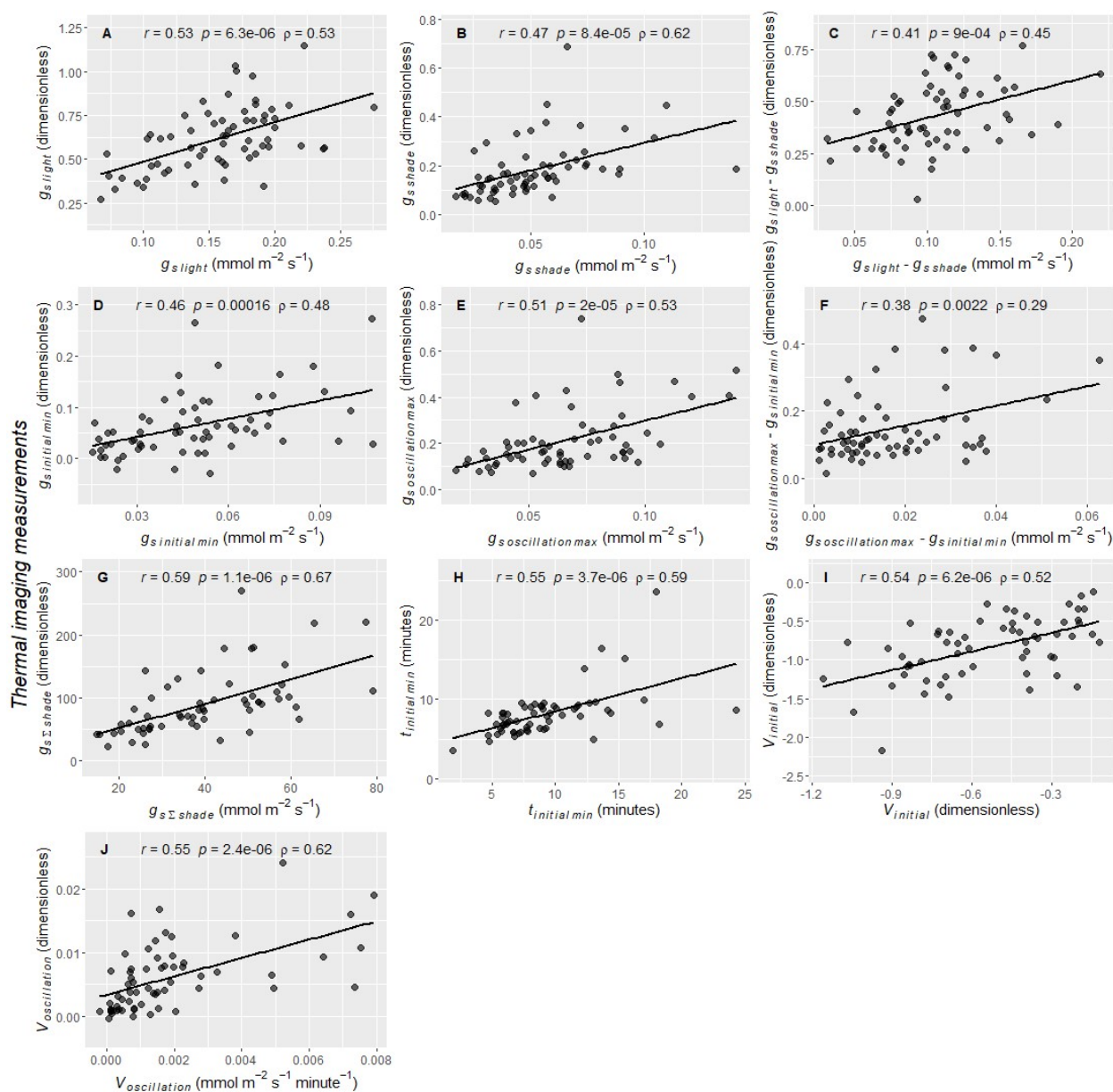
1059 **Zhu XG, Ort DR, Whitmarsh J, Long SP** (2004) The slow reversibility of photosystem II thermal energy dissipation on transfer from
1060 high to low light may cause large losses in carbon gain by crop canopies: a theoretical analysis. *Journal of Experimental*
1061 *Botany* **55**: 1167-1175

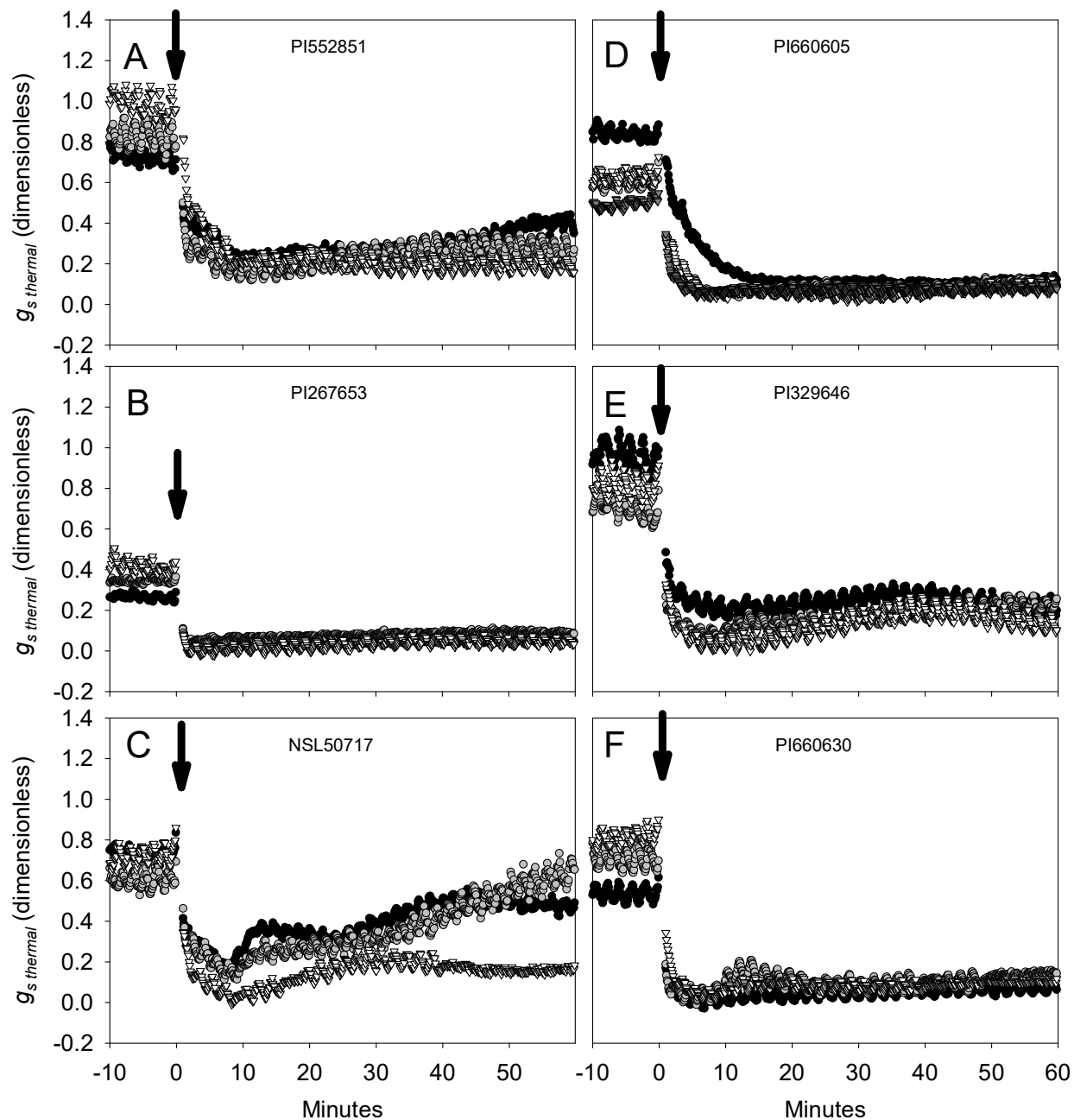
1062

1063



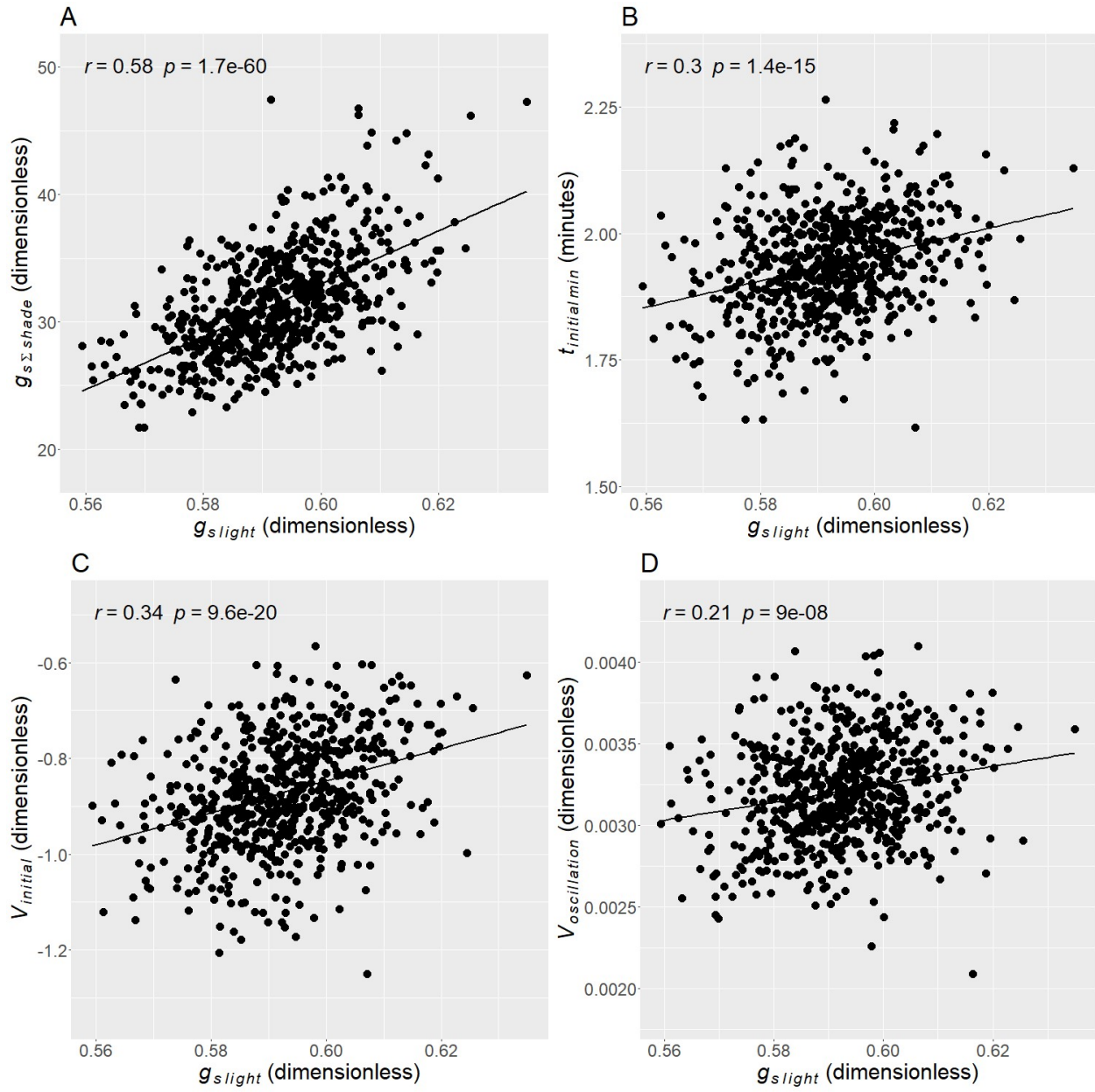


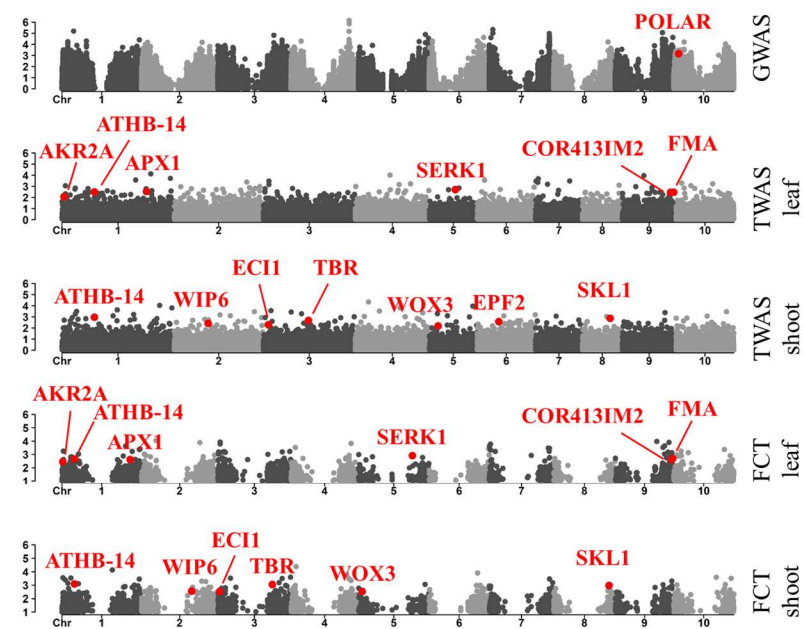
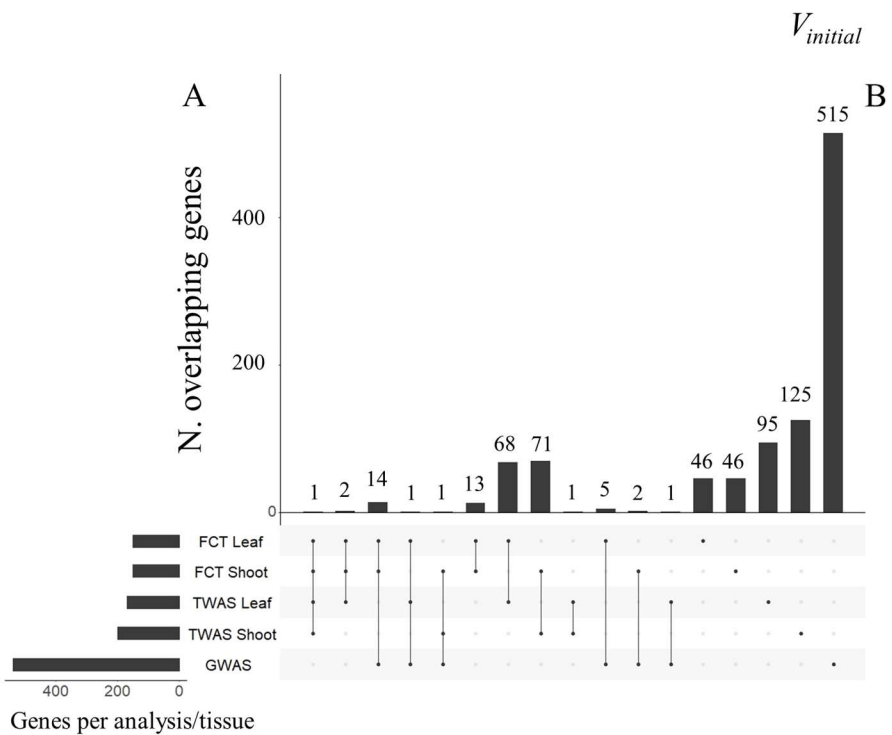


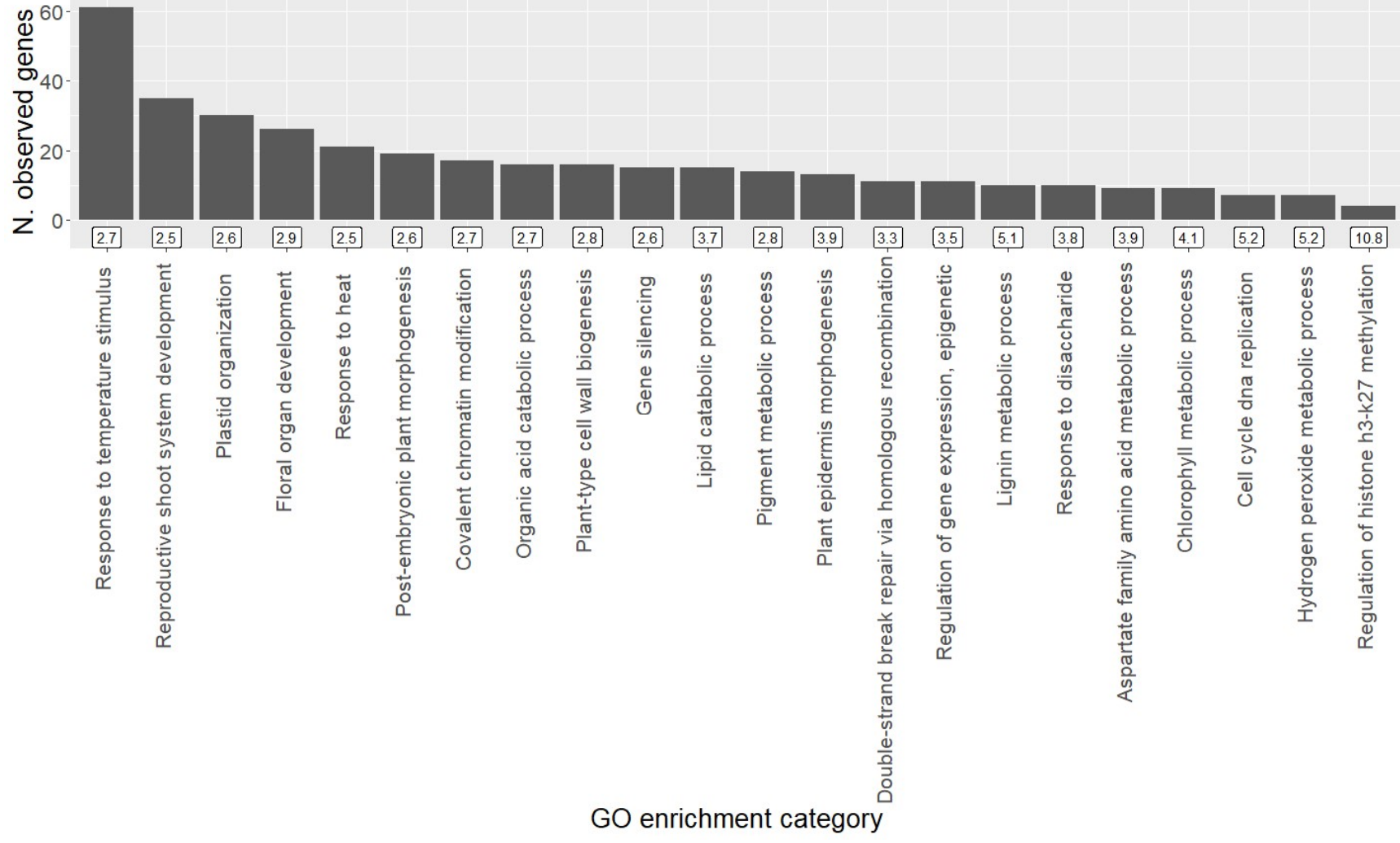


Accession	g_s <i>light</i>	g_s <i>shade</i>	g_s <i>light</i> – g_s <i>shade</i>	g_s <i>initial</i> <i>min</i>	g_s <i>oscillation</i> <i>max</i>	g_s <i>oscillation max</i> – g_s <i>initial min</i>	$t_{initial}$ <i>min</i>	$g_s \Sigma$ <i>shade</i>	$V_{initial}$	$V_{oscillation}$
NSL50717	0.69	0.42	0.27	0.09	0.32	0.23	5.6	179	-0.76	0.021
PI267653	0.34	0.06	0.28	0.01	0.09	0.08	2.4	30	-1.58	0.001
PI329646	0.81	0.20	0.61	0.07	0.26	0.19	4.9	106	-0.96	0.008
PI552851	0.84	0.29	0.55	0.18	0.36	0.18	7.5	150	-0.41	0.003
PI660605	0.64	0.10	0.54	0.05	0.11	0.06	6.1	58	-0.48	0.003
PI660630	0.69	0.11	0.58	-0.01	0.15	0.16	3.4	47	-1.22	0.010









Parsed Citations

Acevedo-Siaca LG, Coe R, Wang Y, Kromdijk J, Quick WP, Long SP (2020) Variation in photosynthetic induction between rice accessions and its potential for improving productivity. *New Phytologist*: 12

Google Scholar: [Author Only](#) [Title Only](#) [Author and Title](#)

Ashburner M, Ball CA, Blake JA, Botstein D, Butler H, Cherry JM, Davis AP, Dolinski K, Dwight SS, Eppig JT, Harris MA, Hill DP, Issel-Tarver L, Kasarskis A, Lewis S, Matese JC, Richardson JE, Ringwald M, Rubin GM, Sherlock G, Gene Ontology C (2000) Gene Ontology: tool for the unification of biology. *Nature Genetics* 25: 25-29

Google Scholar: [Author Only](#) [Title Only](#) [Author and Title](#)

Assmann SM, Jegla T (2016) Guard cell sensory systems: recent insights on stomatal responses to light, abscisic acid, and CO₂. *Current Opinion in Plant Biology* 33: 157-167

Google Scholar: [Author Only](#) [Title Only](#) [Author and Title](#)

Assmann SM, Shimazaki K (1999) The multisensory guard cell. Stomatal responses to blue light and abscisic acid. *Plant Physiology* 119: 809-815

Google Scholar: [Author Only](#) [Title Only](#) [Author and Title](#)

Ball JT, Woodrow IE, Berry JAB (1987) A model predicting stomatal conductance and its contribution to the control of photosynthesis under different environmental conditions. In J Biggins, ed, *Progress in photosynthesis research*. Springer Netherlands, pp 221-224

Google Scholar: [Author Only](#) [Title Only](#) [Author and Title](#)

Ballard T, Peak D, Mott K (2019) Blue and red light effects on stomatal oscillations. *Functional Plant Biology* 46: 146-151

Google Scholar: [Author Only](#) [Title Only](#) [Author and Title](#)

Bernal-Vasquez AM, Utz HF, Piepho HP (2016) Outlier detection methods for generalized lattices: a case study on the transition from ANOVA to REML. *Theoretical and Applied Genetics* 129: 787-804

Google Scholar: [Author Only](#) [Title Only](#) [Author and Title](#)

Boyer JS (1982) Plant productivity and environment. *Science* 218: 443-448

Google Scholar: [Author Only](#) [Title Only](#) [Author and Title](#)

Bradbury PJ, Zhang Z, Kroon DE, Casstevens TM, Ramdoss Y, Buckler ES (2007) TASSEL: software for association mapping of complex traits in diverse samples. *Bioinformatics* 23: 2633-2635

Google Scholar: [Author Only](#) [Title Only](#) [Author and Title](#)

Brodribb TJ, Jordan GJ (2011) Water supply and demand remain balanced during leaf acclimation of *Nothofagus cunninghamii* trees. *New Phytologist* 192(2): 437-448

Google Scholar: [Author Only](#) [Title Only](#) [Author and Title](#)

Browning BL, Browning SR (2016) Genotype Imputation with Millions of Reference Samples. *American Journal of Human Genetics* 98: 116-126

Google Scholar: [Author Only](#) [Title Only](#) [Author and Title](#)

Burks PS, Kaiser CM, Hawkins EM, Brown PJ (2015) Genomewide Association for Sugar Yield in Sweet Sorghum. *Crop Science* 55: 2138-2148

Google Scholar: [Author Only](#) [Title Only](#) [Author and Title](#)

Butler DG, Cullis BR, Gilmour AR, Gogel BJ (2009) *ASReml-R reference manual*. The State of Queensland, Department of Primary Industries and Fisheries, Brisbane .

Google Scholar: [Author Only](#) [Title Only](#) [Author and Title](#)

Carbon S, Douglass E, Dunn N, Good B, Harris NL, Lewis SE, Mungall CJ, Basu S, Chisholm RL, Dodson RJ, Hartline E, Fey P, Thomas PD, Albou LP, Ebert D, Kesling MJ, Mi H, Muruganujan A, Huang X, Poudel S, Mushayahama T, Hu JC, LaBonte SA, Siegele DA, Antonazzo G, Attrill H, Brown NH, Fexova S, Garapati P, Jones TEM, Marygold SJ, Millburn GH, Rey AJ, Trovisco V, dos Santos G, Emmert DB, Falls K, Zhou P, Goodman JL, Strelets VB, Thurmond J, Courtot M, Osumi-Sutherland D, Parkinson H, Roncaglia P, Acencio ML, Kuiper M, Laegreid A, Logie C, Lovering RC, Huntley RP, Denny P, Campbell NH, Kramarz B, Acquah V, Ahmad SH, Chen H, Rawson JH, Chibucos MC, Giglio M, Nadendla S, Tauber R, Duesbury MJ, Del-Toro N, Meldal BHM, Perfetto L, Porras P, Orchard S, Shrivastava A, Xie Z, Chang HY, Finn RD, Mitchell AL, Rawlings ND, Richardson L, Sangrador-Vegas A, Blake JA, Christie KR, Dolan ME, Drabkin HJ, Hill DP, Ni L, Sitnikov D, Harris MA, Oliver SG, Ruther-Ford K, Wood V, Hayles J, Bahler J, Lock A, Bolton ER, De Pons J, Dwinell M, Hayman GT, Laulederkind SJF, Shimoyama M, Tutaj M, Wang SJ, D'Eustachio P, Matthews L, Balhoff JP, Aleksander SA, Binkley G, Dunn BL, Cherry JM, Engel SR, Gondwe F, Karra K, MacPherson KA, Miyasato SR, Nash RS, Ng PC, Sheppard TK, Shrivatsav VPA, Simson M, Skrzypek MS, Weng S, Wong ED, Feuermann M, Gaudet P, Bakker E, Berardini TZ, Reiser L, Subramaniam S, Huala E, Arighi C, Auchincloss A, Axelsen K, Argoud-Puy G, Bateman A, Bely B, Blatter MC, Boutet E, Breuza L, Bridge A, Britto R, Bye-A-Jee H, Casals-Casas C, Coudert E, Estreicher A, Fannigietti L, Garmiri P, Georgiou G, Gos A, Gruaz-Gumowski N, Hatton-Ellis E, Hinz U, Hulo C, Ignatchenko A, Jungo F, Keller G, Laiho K, Lemercier P, Lieberherr D, Lussi Y, Mac-Dougall A, Magrane M, Martin MJ, Masson P, Natale DA, Hyka-Nouspikel N, Pedruzzi I, Pichler K, Poux S, Rivoire C, Rodriguez-Lopez M, Sawford T, Speretta E, Shypitsyna A, Stutz A, Sundaram S, Tognolli M, Tyagi N, Warner K, Zaru R, Wu C, Diehl AD, Chan J, Cho J, Gao S, Grove C, Harrison MC, Howe K, Lee R, Mendel J, Muller HM, Raciti D, Van Auken K, Berriman M, Stein L, Sternberg PW, Howe D, Toro S, Westerfield M, Gene Ontology C (2019) The Gene Ontology Resource: 20 years and still GOing strong. *Nucleic Acids Research* 47: D330-D338

Google Scholar: [Author Only](#) [Title Only](#) [Author and Title](#)

Casa AM, Pressoir G, Brown PJ, Mitchell SE, Rooney WL, Tuinstra MR, Franks CD, Kresovich S (2008) Community resources and strategies for association mapping in sorghum. *Crop Science* 48: 30-40

Google Scholar: [Author Only](#) [Title Only](#) [Author and Title](#)

Chang CC, Chow CC, Tellier L, Vattikuti S, Purcell SM, Lee JJ (2015) Second-generation PLINK: rising to the challenge of larger and richer datasets. *Gigascience* 4: 16

Google Scholar: [Author Only](#) [Title Only](#) [Author and Title](#)

de los Campos G, Sorensen D, Gianola D (2015) Genomic Heritability: What Is It? *Plos Genetics* 11: 21

De Souza AP, Wang Y, Orr DJ, Carmo-Silva E, Long SP (2020) Photosynthesis across African cassava germplasm is limited by Rubisco and mesophyll conductance at steady state, but by stomatal conductance in fluctuating light. *New Phytologist* 225: 2498-2512

Google Scholar: [Author Only](#) [Title Only](#) [Author and Title](#)

Deans RM, Brodribb TJ, Busch FA, Farquhar GD (2019) Plant water-use strategy mediates stomatal effects on the light induction of photosynthesis. *New Phytologist* 222: 382-395

Google Scholar: [Author Only](#) [Title Only](#) [Author and Title](#)

DeLucia EH, Chen S, Guan K, Peng B, Li Y, Gomez-Casanovas N, Kantola IB, Bernacchi CJ, Huang Y, Long SP, Ort DR (2019) Are we approaching a water ceiling to maize yields in the United States? *Ecosphere* 10(6)

dos Santos JPR, Fernandes SB, McCoy S, Lozano R, Brown PJ, Leakey ADB, Buckler ES, Garcia AAF, Gore MA (2020) Novel Bayesian Networks for Genomic Prediction of Developmental Traits in Biomass Sorghum. *G3-Genes Genomes Genetics* 10: 769-781

Google Scholar: [Author Only](#) [Title Only](#) [Author and Title](#)

Dow GJ, Bergmann DC, Berry JA (2014) An integrated model of stomatal development and leaf physiology. *New Phytologist* 201: 1218-1226

Google Scholar: [Author Only](#) [Title Only](#) [Author and Title](#)

Doyle J, Doyle J (1987) A rapid procedure for DNA purification from small quantities of fresh leaf tissue. *Phytochemical Bulletin* 19: 11-15

Google Scholar: [Author Only](#) [Title Only](#) [Author and Title](#)

Durand M, Brendel O, Bure C, Le Thiec D (2019) Altered stomatal dynamics induced by changes in irradiance and vapour-pressure deficit under drought: impacts on the whole-plant transpiration efficiency of poplar genotypes. *New Phytologist* 222: 1789-1802

Google Scholar: [Author Only](#) [Title Only](#) [Author and Title](#)

Edwards EJ, Osborne CP, Stromberg CAE, Smith SA, Bond WJ, Christin PA, Cousins AB, Duvall MR, Fox DL, Freckleton RP, Ghannoum O, Hartwell J, Huang YS, Janis CM, Keeley JE, Kellogg EA, Knapp AK, Leakey ADB, Nelson DM, Saarela JM, Sage RF, Sala OE, Salamin N, Still CJ, Tiplle B, Consortium CG (2010) The Origins of C4 Grasslands: Integrating Evolutionary and Ecosystem Science. *Science* 328: 587-591

Google Scholar: [Author Only](#) [Title Only](#) [Author and Title](#)

Elshire RJ, Glaubitz JC, Sun Q, Poland JA, Kawamoto K, Buckler ES, Mitchell SE (2011) A Robust, Simple Genotyping-by-Sequencing (GBS) Approach for High Diversity Species. *Plos One* 6: 10

Google Scholar: [Author Only](#) [Title Only](#) [Author and Title](#)

Endelman JB, Jannink JL (2012) Shrinkage Estimation of the Realized Relationship Matrix. *G3-Genes Genomes Genetics* 2: 1405-1413

Google Scholar: [Author Only](#) [Title Only](#) [Author and Title](#)

Fahlgren N, Feldman M, Gehan MA, Wilson MS, Shyu C, Bryant DW, Hill ST, McEntee CJ, Warnasooriya SN, Kumar I, Ficor T, Turnipseed S, Gilbert KB, Brutnell TP, Carrington JC, Mockler TC, Baxter I (2015) A Versatile Phenotyping System and Analytics Platform Reveals Diverse Temporal Responses to Water Availability in Setaria. *Molecular Plant* 8: 1520-1535

Google Scholar: [Author Only](#) [Title Only](#) [Author and Title](#)

FAO, IFAD, UNICEF, WFP, WHO (2018) The State of Food Security and Nutrition in the World 2018. Building climate resilience for food security and nutrition. In. FAO, Rome, p 202

Google Scholar: [Author Only](#) [Title Only](#) [Author and Title](#)

Faralli M, Matthews J, Lawson T (2019) Exploiting natural variation and genetic manipulation of stomatal conductance for crop improvement. *Current Opinion in Plant Biology* 49: 1-7

Google Scholar: [Author Only](#) [Title Only](#) [Author and Title](#)

JF Ferguson, SB Fernandes, B Monier, ND Miller, D Allen, A Dmitrieva, P Schmuker, R Lozano, R Valluru, ES Buckler, MA Gore, PJ Brown, EP Spalding, ADB Leakey (2021) Machine learning enabled phenotyping for GWAS and TWAS of WUE traits in 869 field-grown sorghum accessions. *Plant Physiology* in press

Google Scholar: [Author Only](#) [Title Only](#) [Author and Title](#)

Filzmoser P, Garrett RG, Reimann C (2005) Multivariate outlier detection in exploration geochemistry. *Computers & Geosciences* 31: 579-587

Google Scholar: [Author Only](#) [Title Only](#) [Author and Title](#)

Franks PJ, Farquhar GD (2007) The mechanical diversity of stomata and its significance in gas-exchange control. *Plant Physiology* 143:

Google Scholar: [Author Only](#) [Title Only](#) [Author and Title](#)

Glaubit JC, Casstevens TM, Lu F, Harriman J, Elshire RJ, Sun Q, Buckler ES (2014) TASSEL-GBS: A High Capacity Genotyping by Sequencing Analysis Pipeline. Plos One 9: 11

Google Scholar: [Author Only](#) [Title Only](#) [Author and Title](#)

Goodstein DM, Shu SQ, Howson R, Neupane R, Hayes RD, Fazo J, Mitros T, Dirks W, Hellsten U, Putnam N, Rokhsar DS (2012) Phytozome: a comparative platform for green plant genomics. Nucleic Acids Research 40: D1178-D1186

Google Scholar: [Author Only](#) [Title Only](#) [Author and Title](#)

Grant OM, Chaves MM, Jones HG (2006) Optimizing thermal imaging as a technique for detecting stomatal closure induced by drought stress under greenhouse conditions. Physiologia Plantarum 127: 507-518

Google Scholar: [Author Only](#) [Title Only](#) [Author and Title](#)

Grant OM, Tronina L, Jones HG, Chaves MM (2007) Exploring thermal imaging variables for the detection of stress responses in grapevine under different irrigation regimes. Journal of Experimental Botany 58: 815-825

Google Scholar: [Author Only](#) [Title Only](#) [Author and Title](#)

Guilioni L, Jones HG, Leinonen I, Lhomme JP (2008) On the relationships between stomatal resistance and leaf temperatures in thermography. Agricultural and Forest Meteorology 148: 1908-1912

Google Scholar: [Author Only](#) [Title Only](#) [Author and Title](#)

Hadebe ST, Modi AT, Mabhaudhi T (2017) Drought Tolerance and Water Use of Cereal Crops: A Focus on Sorghum as a Food Security Crop in Sub-Saharan Africa. Journal of Agronomy and Crop Science 203: 177-191

Google Scholar: [Author Only](#) [Title Only](#) [Author and Title](#)

Hetherington AM, Woodward FI (2003) The role of stomata in sensing and driving environmental change. Nature 424: 901-908

Google Scholar: [Author Only](#) [Title Only](#) [Author and Title](#)

Jones HG (1999) Use of infrared thermometry for estimation of stomatal conductance as a possible aid to irrigation scheduling. Agricultural and Forest Meteorology 95: 139-149

Google Scholar: [Author Only](#) [Title Only](#) [Author and Title](#)

Jones HG, Stoll M, Santos T, de Sousa C, Chaves MM, Grant OM (2002) Use of infrared thermography for monitoring stomatal closure in the field: application to grapevine. Journal of Experimental Botany 53: 2249-2260

Google Scholar: [Author Only](#) [Title Only](#) [Author and Title](#)

Kaiser E, Morales A, Harbinson J (2018) Fluctuating Light Takes Crop Photosynthesis on a Rollercoaster Ride. Plant Physiology 176: 977-989

Google Scholar: [Author Only](#) [Title Only](#) [Author and Title](#)

Kaiser E, Morales A, Harbinson J, Kromdijk J, Heuvelink E, Marcelis LFM (2015) Dynamic photosynthesis in different environmental conditions. Journal of Experimental Botany 66: 2415-2426

Google Scholar: [Author Only](#) [Title Only](#) [Author and Title](#)

Kaiser H, Kappen L (2001) Stomatal oscillations at small apertures: indications for a fundamental insufficiency of stomatal feedback-control inherent in the stomatal turgor mechanism. Journal of Experimental Botany 52: 1303-1313

Google Scholar: [Author Only](#) [Title Only](#) [Author and Title](#)

Kerstiens G (1996) Cuticular water permeability and its physiological significance. Journal of Experimental Botany 47: 1813-1832

Google Scholar: [Author Only](#) [Title Only](#) [Author and Title](#)

Koester RP, Nohl BM, Diers BW, Ainsworth EA (2016) Has photosynthetic capacity increased with 80 years of soybean breeding? An examination of historical soybean cultivars. Plant Cell and Environment 39: 1058-1067

Google Scholar: [Author Only](#) [Title Only](#) [Author and Title](#)

Kreming KAG, Diepenbrock CH, Gore MA, Buckler ES, Bandillo NB (2019) Transcriptome-Wide Association Supplements Genome-Wide Association in Zea mays. G3-Genes Genomes Genetics 9: 3023-3033

Google Scholar: [Author Only](#) [Title Only](#) [Author and Title](#)

Langmead B, Salzberg SL (2012) Fast gapped-read alignment with Bowtie 2. Nature Methods 9: 357-U354

Google Scholar: [Author Only](#) [Title Only](#) [Author and Title](#)

Lawson T, Blatt MR (2014) Stomatal Size, Speed, and Responsiveness Impact on Photosynthesis and Water Use Efficiency. Plant Physiology 164: 1556-1570

Google Scholar: [Author Only](#) [Title Only](#) [Author and Title](#)

Lawson T, Violet-Chabrand S (2019) Speedy stomata, photosynthesis and plant water use efficiency. New Phytologist 221: 93-98

Google Scholar: [Author Only](#) [Title Only](#) [Author and Title](#)

Lawson T, von Caemmerer S, Baroli I (2011) Photosynthesis and Stomatal Behaviour. In U Luttge, W Beyschlag, B Budel, D Francis, eds, Progress in Botany 72, Vol 72. Springer-Verlag Berlin, Berlin, pp 265-304

Google Scholar: [Author Only](#) [Title Only](#) [Author and Title](#)

Leakey ADB, Ferguson JN, Pignion CP, Wu A, Jin Z, Hammer GL, Lobell DB (2019) Water use efficiency as a constraint and target for improving the resilience and productivity of C3 and C4 crops. *Annual Review of Plant Biology* 70: 781-808

Google Scholar: [Author Only](#) [Title Only](#) [Author and Title](#)

Liu HJ, Yan JB (2019) Crop genome-wide association study: a harvest of biological relevance. *Plant Journal* 97: 8-18

Google Scholar: [Author Only](#) [Title Only](#) [Author and Title](#)

Lobell DB, Burke MB, Tebaldi C, Mastrandrea MD, Falcon WP, Naylor RL (2008) Prioritizing climate change adaptation needs for food security in 2030. *Science* 319: 607-610

Google Scholar: [Author Only](#) [Title Only](#) [Author and Title](#)

Lobell DB, Roberts MJ, Schlenker W, Braun N, Little BB, Rejesus RM, Hammer GL (2014) Greater Sensitivity to Drought Accompanies Maize Yield Increase in the US Midwest. *Science* 344: 516-519

Google Scholar: [Author Only](#) [Title Only](#) [Author and Title](#)

McAdam SAM, Brodribb TJ (2015) The Evolution of Mechanisms Driving the Stomatal Response to Vapor Pressure Deficit. *Plant Physiology* 167: 833-843

Google Scholar: [Author Only](#) [Title Only](#) [Author and Title](#)

McAusland L, Davey PA, Kanwal N, Baker NR, Lawson T (2013) A novel system for spatial and temporal imaging of intrinsic plant water use efficiency. *Journal of Experimental Botany* 64: 4993-5007

Google Scholar: [Author Only](#) [Title Only](#) [Author and Title](#)

McAusland L, Viallet-Chabrand S, Davey P, Baker NR, Brendel O, Lawson T (2016) Effects of kinetics of light-induced stomatal responses on photosynthesis and water-use efficiency. *New Phytologist* 211: 1209-1220

Google Scholar: [Author Only](#) [Title Only](#) [Author and Title](#)

Merlot S, Mustilli AC, Genty B, North H, Lefebvre V, Sotta B, Vavasseur A, Giraudat J (2002) Use of infrared thermal imaging to isolate *Arabidopsis* mutants defective in stomatal regulation. *Plant Journal* 30: 601-609

Google Scholar: [Author Only](#) [Title Only](#) [Author and Title](#)

Mi HY, Muruganujan A, Ebert D, Huang XS, Thomas PD (2019) PANTHER version 14: more genomes, a new PANTHER GO-slim and improvements in enrichment analysis tools. *Nucleic Acids Research* 47: D419-D426

Google Scholar: [Author Only](#) [Title Only](#) [Author and Title](#)

Morris GP, Ramu P, Deshpande SP, Hash CT, Shah T, Upadhyaya HD, Riera-Lizarazu O, Brown PJ, Acharya CB, Mitchell SE, Harriman J, Glaubitz JC, Buckler ES, Kresovich S (2013) Population genomic and genome-wide association studies of agroclimatic traits in sorghum. *Proceedings of the National Academy of Sciences of the United States of America* 110: 453-458

Google Scholar: [Author Only](#) [Title Only](#) [Author and Title](#)

Nunes TDG, Zhang D, Raissig MT (2020) Form, development and function of grass stomata. *Plant Journal* 101: 780-799

Google Scholar: [Author Only](#) [Title Only](#) [Author and Title](#)

Ort DR, Long SP (2014) Limits on Yields in the Corn Belt. *Science* 344: 483-484

Google Scholar: [Author Only](#) [Title Only](#) [Author and Title](#)

Ortiz D, Hu JY, Fernandez MGS (2017) Genetic architecture of photosynthesis in *Sorghum bicolor* under non-stress and cold stress conditions. *Journal of Experimental Botany* 68: 4545-4557

Google Scholar: [Author Only](#) [Title Only](#) [Author and Title](#)

Papanatsiou M, Petersen J, Henderson L, Wang Y, Christie JM, Blatt MR (2019) Optogenetic manipulation of stomatal kinetics improves carbon assimilation, water use, and growth. *Science* 363: 1456-+

Google Scholar: [Author Only](#) [Title Only](#) [Author and Title](#)

Paterson AH, Bowers JE, Bruggmann R, Dubchak I, Grimwood J, Gundlach H, Haberer G, Hellsten U, Mitros T, Poliakov A, Schmutz J, Spannagl M, Tang HB, Wang XY, Wicker T, Bharti AK, Chapman J, Feltus FA, Gowik U, Grigoriev IV, Lyons E, Maher CA, Martis M, Narechania A, Otillar RP, Penning BW, Salamov AA, Wang Y, Zhang LF, Carpita NC, Freeling M, Gingle AR, Hash CT, Keller B, Klein P, Kresovich S, McCann MC, Ming R, Peterson DG, Mehboob ur R, Ware D, Westhoff P, Mayer KFX, Messing J, Rokhsar DS (2009) The *Sorghum bicolor* genome and the diversification of grasses. *Nature* 457: 551-556

Google Scholar: [Author Only](#) [Title Only](#) [Author and Title](#)

Pearcy RW (1990) Sunflecks and photosynthesis in plant canopies. *Annual Review of Plant Physiology and Plant Molecular Biology* 41: 421-453

Google Scholar: [Author Only](#) [Title Only](#) [Author and Title](#)

Pignion CP (2017) Strategies to improve C4 photosynthesis, water and resource-use efficiency under different atmospheres, temperatures, and light environments. University of Illinois at Urbana-Champaign, Urbana, Illinois

Google Scholar: [Author Only](#) [Title Only](#) [Author and Title](#)

Pignion CP, Leakey ADB, Long SP, Kromdijk J (2021) Drivers of Natural Variation in Water-Use Efficiency Under Fluctuating Light Are Promising Targets for Improvement in Sorghum. *Frontiers in Plant Science* 12: 13

Google Scholar: [Author Only](#) [Title Only](#) [Author and Title](#)

PT Prakash, D Banan, RE Paul, MJ Feldman, D Xie, L Freyfogle, I Baxter, ADB Leakey (2021) Correlation and co-localization of QTL for stomatal density and canopy temperature under drought stress in *Setaria*. *Journal of Experimental Botany* (in press).

Google Scholar: [Author Only](#) [Title Only](#) [Author and Title](#)

R Core Team (2017) R: A language and environment for statistical computing., R Foundation for Statistical Computing, Vienna, Australia

Ray DK, Mueller ND, West PC, Foley JA (2013) Yield Trends Are Insufficient to Double Global Crop Production by 2050. *Plos One* 8: 8

Google Scholar: [Author Only](#) [Title Only](#) [Author and Title](#)

Regassa TH, Wortmann CS (2014) Sweet sorghum as a bioenergy crop: Literature review. *Biomass & Bioenergy* 64: 348-355

Google Scholar: [Author Only](#) [Title Only](#) [Author and Title](#)

Remm M, Storm CEV, Sonnhammer ELL (2001) Automatic clustering of orthologs and in-paralogs from pairwise species comparisons. *Journal of Molecular Biology* 314: 1041-1052

Google Scholar: [Author Only](#) [Title Only](#) [Author and Title](#)

Sagan V, Maimaitijiang M, Sidike P, Eblimit K, Peterson KT, Hartling S, Esposito F, Khanal K, Newcomb M, Pauli D, Ward R, Fritschi F, Shakoor N, Mockler T (2019) UAV-Based High Resolution Thermal Imaging for Vegetation Monitoring, and Plant Phenotyping Using ICI 8640 P, FLIR Vue Pro R 640, and thermoMap Cameras. *Remote Sensing* 11

Google Scholar: [Author Only](#) [Title Only](#) [Author and Title](#)

Serna L (2011) Stomatal development in *Arabidopsis* and grasses: differences and commonalities. *International Journal of Developmental Biology* 55: 5-10

Google Scholar: [Author Only](#) [Title Only](#) [Author and Title](#)

Shimazaki K, Doi M, Assmann SM, Kinoshita T (2007) Light regulation of stomatal movement. *Annual Review of Plant Biology* 58: 219-247

Google Scholar: [Author Only](#) [Title Only](#) [Author and Title](#)

Sinclair TR, Tanner CB, Bennett JM (1984) Water-use efficiency in crop production. *Bioscience* 34: 36-40

Google Scholar: [Author Only](#) [Title Only](#) [Author and Title](#)

Soleh MA, Tanaka Y, Nomoto Y, Iwahashi Y, Nakashima K, Fukuda Y, Long SP, Shiraiwa T (2016) Factors underlying genotypic differences in the induction of photosynthesis in soybean *Glycine max* (L.) Merr. *Plant Cell and Environment* 39: 685-693

Google Scholar: [Author Only](#) [Title Only](#) [Author and Title](#)

Stegle O, Parts L, Durbin R, Winn J (2010) A Bayesian Framework to Account for Complex Non-Genetic Factors in Gene Expression Levels Greatly Increases Power in eQTL Studies. *Plos Computational Biology* 6: 11

Google Scholar: [Author Only](#) [Title Only](#) [Author and Title](#)

Takahashi S, Monda K, Negi J, Konishi F, Ishikawa S, Hashimoto-Sugimoto M, Goto N, Iba K (2015) Natural Variation in Stomatal Responses to Environmental Changes among *Arabidopsis thaliana* Ecotypes. *Plos One* 10: 13

Google Scholar: [Author Only](#) [Title Only](#) [Author and Title](#)

Tam V, Patel N, Turcotte M, Bosse Y, Pare G, Meyre D (2019) Benefits and limitations of genome-wide association studies. *Nature Reviews Genetics* 20: 467-484

Google Scholar: [Author Only](#) [Title Only](#) [Author and Title](#)

Valluru R, Gazave EE, Fernandes SB, Ferguson JN, Lozano R, Hirannaiah P, Zuo T, Brown PJ, Leakey ADB, Gore MA, Buckler ES, Bandillo N (2019) Deleterious Mutation Burden and Its Association with Complex Traits in Sorghum (*Sorghum bicolor*). *Genetics* 211: 1075-1087

Google Scholar: [Author Only](#) [Title Only](#) [Author and Title](#)

Violet-Chabrand S, Lawson T (2019) Dynamic leaf energy balance: deriving stomatal conductance from thermal imaging in a dynamic environment. *Journal of Experimental Botany* 70: 2839-2855

Google Scholar: [Author Only](#) [Title Only](#) [Author and Title](#)

Vico G, Manzoni S, Palmroth S, Katul G (2011) Effects of stomatal delays on the economics of leaf gas exchange under intermittent light regimes. *New Phytologist* 192: 640-652

Google Scholar: [Author Only](#) [Title Only](#) [Author and Title](#)

von Caemmerer S, Farquhar GD (1981) Some relationships between the biochemistry of photosynthesis and the gas exchange of leaves. *Planta* 153: 376-387

Google Scholar: [Author Only](#) [Title Only](#) [Author and Title](#)

Wang Y, Burgess SJ, de Becker EM, Long SHP (2020) Photosynthesis in the fleeting shadows: an overlooked opportunity for increasing crop productivity? *Plant Journal* 101: 874-884

Google Scholar: [Author Only](#) [Title Only](#) [Author and Title](#)

Way DA, Pearcy RW (2012) Sunflecks in trees and forests: from photosynthetic physiology to global change biology. *Tree Physiology* 32: 1066-1081

Google Scholar: [Author Only](#) [Title Only](#) [Author and Title](#)

Wei T, Simko V (2017) R package "corrplot": Visualization of a Correlation Matrix. In,

Google Scholar: [Author Only](#) [Title Only](#) [Author and Title](#)

Wong SC, Cowan IR, Farquhar GD (1979) Stomatal conductance correlates with photosynthetic capacity. Nature 282: 424-426

Google Scholar: [Author Only](#) [Title Only](#) [Author and Title](#)

WWAP (2015) The United Nations world water development report 2015: Water for a sustainable world. In. UNESCO, Paris

Google Scholar: [Author Only](#) [Title Only](#) [Author and Title](#)

Zhou X, Stephens M (2012) Genome-wide efficient mixed-model analysis for association studies. Nature Genetics 44: 821-U136

Google Scholar: [Author Only](#) [Title Only](#) [Author and Title](#)

Zhou X, Stephens M (2014) Efficient multivariate linear mixed model algorithms for genome-wide association studies. Nature Methods 11: 407-+

Google Scholar: [Author Only](#) [Title Only](#) [Author and Title](#)

Zhou XY, Huang XH (2019) Genome-wide Association Studies in Rice: How to Solve the Low Power Problems? Molecular Plant 12: 10-12

Google Scholar: [Author Only](#) [Title Only](#) [Author and Title](#)

Zhu XG, Ort DR, Whitmarsh J, Long SP (2004) The slow reversibility of photosystem II thermal energy dissipation on transfer from high to low light may cause large losses in carbon gain by crop canopies: a theoretical analysis. Journal of Experimental Botany 55: 1167-1175

Google Scholar: [Author Only](#) [Title Only](#) [Author and Title](#)